https://doi.org/10.5194/egusphere-2026-1045
Preprint. Discussion started: 10 March 2026

Persistent episodes of the Euro-Atlantic upper-level jets in summer: precursors, maintainers and impacts.

Hugo Banderier[1], Tim Woollings[2], and Olivia Martius[1,3]

[1]Institute of Geography and Oeschger Center for Climate Change Research, University of Bern, Bern, Switzerland
[2]Atmospheric, Oceanic and Planetary Physics, University of Oxford, Oxford, United Kingdom
[3]Mobiliar Lab for Natural Risks, University of Bern, Bern, Switzerland

Correspondence: Hugo Banderier (hugo.banderier@unibe.ch)

Abstract. Recent studies have highlighted the link between upper-level jet stream dynamics, especially the persistence of certain jet configurations, and extreme summer weather in Europe. In this work, we use a recently developed toolbox for the detection and study of jet core features in wind speed fields to define persistent episodes of the subtropical or of the eddy-driven jet over the Euro-Atlantic sector and focusing on summer. During these events, we analyse the state of the jets themselves, as well as of the atmosphere directly surrounding the jet, using jet-centred composites. We study the role of these quantities as potential precursors to, or maintainers of persistent episodes. Fields used to quantify the state of the atmosphere before or during persistent episodes include events of high variability or high persistence like Rossby wave breaking or blocks, and potential sources or sinks of momentum such as temperature gradient, diabatic processes or eddy activity. We also systematically study the link between these episodes and severe weather events in Europe.

We show that the two jet categories have different persistence properties and persistent episode temporal distribution. The precursors, maintainers and impacts of these events are also vastly different, although commonalities exist. Both jets are, on average over their persistent episodes, stronger and shifted equatorward compared to their summer mean state. Looking into each individual episode reveals that each jet's persistence can be explained using a combination mechanisms, which include both remote, large-scale drivers as well as local effects. We a significant increase in hot and dry spells during persistent episodes of the STJ, and of wet spells during persistent episodes of the EDJ.

1 Introduction

Jet streams and Rossby waves have been identified as central large scale drivers of surface impacts in the mid latitudes (e.g., Schubert et al., 2011; Winters and Martin, 2014; Harnik et al., 2016; White et al., 2022) and in Europe, unusual and persistent configurations of the jets have been shown to co-occur with persistent or recurrent surface extreme events such as Eurasian heat waves (Röthlisberger et al., 2016; Rousi et al., 2022), warm, cold or wet extremes in the European winter (Pinto et al., 2014; Schaller et al., 2016; Priestley et al., 2017; Kopp et al., 2021; Galfi and Messori, 2023). However, these studies either do not quantify jet persistence, or define it using a scalar proxy such as the jet's preferred latitude. There are open questions if these proxies cover all angles of jet persistence, and if the hypothesis suggested by these case studies that persistent jets can force

https://doi.org/10.5194/egusphere-2026-1045
Preprint. Discussion started: 10 March 2026

persistent surface conditions holds systematically. To address these questions, we briefly summarise the current understanding of atmospheric persistence, and connect it to the jet stream.

Persistence is not uniquely defined and the term is used in different contexts in large scale dynamics and extreme events research Tuel and Martius (2023). The term is used for example in reference to the duration or stationarity of flow patterns such as weather regimes (e.g., Vautard, 1990), in reference to recurring flow configurations (e.g., Tuel and Martius, 2023), or in the context of dynamical system theory (e.g., Messori et al., 2017). Here we focus exclusively on stationarity and episodic persistence and ignore recurrence, such that the words "persistence" and "stationarity" are used interchangeably. In the literature, jet persistence is typically studied via a singular aspect. It is either an index, typically representing the jet's preferred latitude (Barnes et al., 2010; Franzke et al., 2011; Galfi and Messori, 2023), or the duration of an identified recurrent and interpretable pattern (Gerber and Vallis, 2007; Rousi et al., 2022). An alternative approach can be found with dynamical systems theory, which can extract a persistence metric out of any higher-dimensional timeseries (in this example geopotential height in a region: Faranda et al., 2017).

To connect the concept of persistence to the jets, we briefly summarise the mechanisms that drive and maintain the two types of jets in our study domain, the subtropical jet (STJ) and the eddy-driven jet (EDJ). Meridional export of tropical momentum and heat by the Hadley cell is the main driver of the the STJ, while momentum flux from synoptic eddies propels the EDJ. Momentum fluxes from Rossby wave breaking (RWB) are part of the self-maintenance of the EDJ, since transient eddies emerge from the baroclinic instability of the EDJ (e.g., Robinson, 2006; Barnes and Hartmann, 2010). Diabatic processes, especially latent heating accompanying precipitation on the equatorward flank of the jet, can enhance these maintenance mechanisms by warming the equatorward flank of the jet, and by creating or strengthening negative PV anomalies on this same flank (Wernli and Gray, 2024; Auestad et al., 2024, 2025). Stronger jets are hypothesised to be less variable in their latitudinal position at the daily timescale (Woollings et al., 2018), and so are equatorward shifted jets (Barnes et al., 2010; Faranda et al., 2017). Therefore any source of additional momentum is a potential driver of jet persistence. A mechanism that is both a source of momentum but also of high variability in jet intensity and position is Rossby wave breaking. The life cycles of baroclinic waves in the mid latitudes terminate with a non-linear breaking after a phase of linear growth (e.g. Thorncroft et al., 1993) that is characterised by overturning of the PV contours on isentropic surfaces, whose orientation defines the type of wave breaking: anticyclonic or cyclonic wave breaking (AWB or CWB McIntyre and Palmer, 1983). AWBs typically happen on the equatorward flank of the jet, and more frequent when the jet is poleward-shifted, and are associated with poleward momentum flux. CWBs are typically associated with longer lasting life cycles, typically happen on the poleward flank of the jet and are associated with equatorward momentum flux (Thorncroft et al., 1993; Martius et al., 2007; Rupp and Birner, 2021). Finally, warm conveyor belt (WCB) outflows can be a source of both momentum flux into the jet and variability. The interaction of WCB outflows with the jet has been shown to be pronounced for poleward shifted jets (Vishnupriya et al., 2025).

Whether they are persistent or not, jet streams influence surface conditions (Trouet et al., 2018; Maddison et al., 2023; García-Burgos et al., 2023; Brönnimann et al., 2025). The eddy-driven jet is co-located with the storm tracks in the mid latitudes, whose position is a major source of weather variability in Europe at sub-seasonal time scale (Buehler et al., 2011) and both jets are linked to the formation, propagation and decay of surface weather systems. A stationary EDJ might therefore

https://doi.org/10.5194/egusphere-2026-1045
Preprint. Discussion started: 10 March 2026

be synonymous with cyclone clustering in this context (Schaller et al., 2016; Dacre and Pinto, 2020; Kopp et al., 2021). Eddies may also maintain and reinforce a blocking anticyclone, a persistent anticyclone typically associated with Rossby wave breaking (Shutts, 1983; Yamazaki and Itoh, 2013; Drouard and Woollings, 2018). This creates persistent conditions for the jet, which deviates around the high pressure system on the poleward or equatorward side of the blocking anticyclone, and for the block, reinforced by eddies but not advected by the jet. Consequently the onset of a blocking event can mark the start of a persistent episode of the jet.

We identify six research questions which are only partially answered by the literature cited above that we aim to explore with this work.

- Q1: Can episodic jet persistence be defined in an objective way, that does not require defining a scalar time series that represents the state of the jet?
- Q2: What are the specific characteristics of persistent jet episodes?
- Q3: When both the STJ and the EDJ are present, what are the characteristics of the other jet when one is persistent?
- Q4: Are persistent jet episodes systematically linked to surface extremes? What pathways can explain these links?
- Q5: What are the atmospheric processes involved in the formation and maintenance of persistent jet episodes?
- Q6 Specifically, what kind of wave breaking (intensity, orientation, location relative to the jet) is beneficial to jet persistence and what kind is detrimental to it?

In this work, we build on the methods introduced in Banderier et al. (2025), namely jet core detection and categorisation, to study long-lasting episodes of high jet stationarity. We focus our analysis on the Euro-Atlantic sector and the northern hemisphere extended summer. This season is known to feature many extreme events linked to atmospheric dynamics (e.g. Drouard et al., 2019), yet the bulk of the research on jet dynamics focuses on winter, when the jets are stronger and more separated from each other.

2 Data and Methods

2.1 Data

The jet cores in the Euro-Atlantic sector ($80\,°\mathrm{W} - 40\,°\mathrm{E}$, $15\,°\mathrm{N} - 80\,°\mathrm{N}$) are detected on fields of upper-level horizontal wind speed (u, v and $U = \sqrt{u^2 + v^2}$) at $0.5°$ spatial resolution from ERA5 (European Center for Medium-range Weather Forecast Reanalysis 5, hereafter ERA5; Hersbach et al., 2020) in the period 1959-2022, in six-hourly time steps between 15 June and 31 September. Two-dimensional fields of u, v and U are created by taking, at each time step and grid point, the value at the pressure level of maximum U across the 175, 200, 225, 250, 300 and $350\,\mathrm{hPa}$ pressure levels.

Additionally, we use geopotential height anomalies at $500\,\mathrm{hPa}$ (Z'_{500}) relative to a 15-day smoothed daily climatology, potential temperature θ on the $2\mathrm{PVU}$ surface (2 potential vorticity unit surface; the isosurface where potential vorticity is equal

https://doi.org/10.5194/egusphere-2026-1045
Preprint. Discussion started: 10 March 2026

to $2\,\mathrm{PVU} = 2 \times 10^{-6}\,\mathrm{m^2 s^{-1}\,Kkg^{-1}}$), potential vorticity (PV) on the $350\,\mathrm{K}$ or $330\,\mathrm{K}$ isentrope (for the STJ and EDJ, respectively), atmospheric temperature at $2\,\mathrm{m}$, daily accumulated precipitation, anticyclonic and cyclonic Rossby wave breaking (RWB) occurrence and blocking occurrence.

Binary 2-D RWB fields are created by first applying the overturning index (Barnes and Hartmann, 2012; Kaderli, 2024) to all isentropes between 310 and $350\,\mathrm{K}$ and increments of $5\,\mathrm{K}$. The overturning index produces, for each isentrope, a 2-D field with zeros everywhere, and will flag with ones every grid point within the smallest rectangular longitude-latitude box that contains the overturning of a chosen PV contour. These fields are then aggregated across the isentropes at each longitude and latitude, by setting the value to 1 if a RWB is detected on any isentrope, otherwise the value is 0. We use the shorthands AWB and CWB for anticyclonic and cyclonic RWB, which are distinguished using the sign of the meridional momentum flux.

The four summer weather regimes (Cassou et al., 2005) are extracted from the Z'_{500} timeseries using the method described in Grams et al. (2017) but restricted to summer. They are named Scandinavian Blocking (SB, named "Blocking" in Cassou et al. 2005), Atlantic Low (AL), Greenland Blocking (GB, named "NAO-" in Cassou et al. 2005), and Atlantic Ridge (AR).

Eddy velocities at 250 hPa (u'_{250}, v'_{250}) are finally extracted from the absolute velocities on this isobar using a 10-day high-pass Lanczos filter. Eddy kinetic energy (EKE) and eddy momentum flux (EMF) convergence are computed from these eddy velocity fields.

2.2 Jet detection and categorisation

The jet cores are one-dimensional features defined as a long- and strong enough, wind-direction-aligned series of points that all are local maxima of wind speed in along the line normal to the velocity vector, and that form a curve. In practice, these curves are obtained as subsets of isolines of zero horizontal normal shear field $\sigma := \frac{\partial U}{\partial n} = \frac{v}{U}\frac{\partial U}{\partial x} - \frac{u}{U}\frac{\partial U}{\partial y}$, where x and y are local Cartesian coordinates.

The jet cores are classified either as eddy-driven jet (EDJ) or subtropical jet (STJ) according to their vertical wind profile and altitude expressed in potential temperature coordinates. Finally, about twenty properties are computed on each jet core such as mean longitude, latitude, pressure level, maximum wind speed, mean instantaneous width, tilt and waviness.

The main output of this algorithm are forty time series, one for each jet property and category. If several jets of a given category are detected within a single time step, the value of a property for this jet category at this time step will be a weighted mean, where the weights are the individual jets' integrated wind speed along the core. Please refer to Banderier et al. (2025) for more details.

2.3 Persistence of the jet

In this section, the objective is to find a metric for jet persistence that is intuitive and stable even under complex situations. We do not explicitly track the jet cores over time. This means we do not try to find, for each jet one or several successors among the jets in the following time step(s) as would approaches like that of Limbach et al. (2012). We instead rely on the already successful jet categorisation to implicitly track the jets. In other words, the successor of one time step's EDJ is always the next

https://doi.org/10.5194/egusphere-2026-1045
Preprint. Discussion started: 10 March 2026

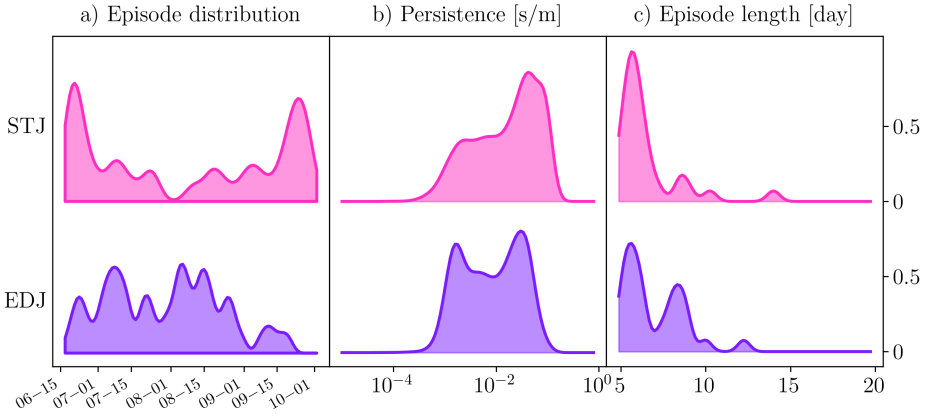

Figure 1. Distribution of persistence and persistence episodes for both categories of jets, smoothed using Gaussian kernel density estimation (KDE) with bandwidths b and scaled arbitrarily. a) Persistent episode occurrence frequency at each ordinal day of extended summer, $b = 0.08$. b) Persistence metric. KDE is performed in log space, using $b = 0.2$. c) Lengths of episodes in days, $b = 0.2$.

time step's EDJ, and likewise for the STJ. This approach was found technically simpler and more stable under complicated situations, especially for a small domain.

For each jet category c (STJ or EDJ) and time step t, we compute the longitudinal overlap o_t^c and distance d_t^c between the jet c at time steps t and $t+1$. The distance metric is the Fréchet distance (see e.g. Alt and Godau, 2011, for a definition) based on the pairwise haversine distances between the points in jet c at time t and the points in the jet c at time $t+1$. We use these two values to compute the simple persistence metric $P_t^c = \frac{\Delta t \times o_t^c}{d_t^c}$, in units of sm^{-1} and where Δt is the amount of time between time steps, six hours in this study. Several alternative distance definitions between curves were tested (a review of such metrics can be found in Jekel et al., 2019) with little changes to the results. When no successor or predecessor exists, the distance is undefined.

A persistent episode of the jet c is finally extracted the same way one would define a heat wave from a temperature time series, based on a quantile threshold and a minimum duration. We set the minimum length to five days and adjust the quantile thresholds to obtain the 30 most persistent episodes of each jet in extended summer, 15 June to 30 September. The results do not change for 20 or 40 episodes, and keeping a moderate number allows us to study each event individually. We show here the seasonal distribution of these persistent episodes for each jet (Figure 1a), as well as the distribution of the persistence metric itself (Figure 1b), and of the lengths of the 30 episodes (Figure 1c). The STJ episodes are more likely to happen at the start or the end of the season, while EDJ episodes happen throughout the year. The persistence metric shows a similar distribution for both jets, with a slight shift to higher persistence values for the STJ. The EDJ has more longer episodes then the STJ although the longest episode, lasting 56 days, is of the STJ.

https://doi.org/10.5194/egusphere-2026-1045
Preprint. Discussion started: 10 March 2026

2.4 Jet-centred composites

Inspired by storm-centred composites (e.g. Frank, 1977; Bengtsson et al., 2007), composites are created in natural coordinates around the position of the instantaneous jet cores in order to study the immediate environment around them, irrespective of the jets' location, orientation and length. They are similar to those seen in Auestad et al. (2024), but taking the position along the jet as the horizontal coordinate as opposed to its local orientation.

This is, in essence, a coordinate change from the longitude – latitude grid to the natural coordinates (tangent and normal to the horizontal wind vector) of the jet of interest, the STJ or the EDJ, found in the same time step. In practice, segments normal to the horizontal wind direction are created around each point of the jet, spanning $2 \times 10^6\,\mathrm{m}$ on each side, discretised by segment points every $1 \times 10^5\,\mathrm{m}$. The two-dimensional field, for example potential temperature on the $2\,\mathrm{PVU}$ surface, is then bi-linearly interpolated onto each segment points, creating a two-dimensional interpolated field of dimensions (# of jet points, # of segment points). To be able to composite several of these interpolated fields, each created around jets of varying lengths, the fields are linearly interpolated once more, this time along the first dimension, onto the $[0, 1]$ domain discretised into thirty evenly spaced points. This will allow for analyses of processes affecting entrance- and exit regions of jets, on their cold- or warm flanks, irrespective of their location, orientation or length. No special consideration is applied in the case of overturning events where the jet locally goes westward, and the cold flank segments in these cases will locally point southward.

Note that the procedure is entirely two-dimensional and does not discriminate the type of 2-D surface the field lies on or its altitude relative to the jet's, so that we may use it to study near-surface fields and column averages when relevant.

By performing this operation on every time step and averaging over years for each calendar day, we can compute daily climatologies of such interpolated fields. The climatologies used to produce the results of this study are smoothed along the time dimension with a 15 calendar days rolling window.

A final layer to this analysis is the crucial importance of the magnitude of the across-jet gradient of some of these variables, namely potential temperature on the $2\,\mathrm{PVU}$ surface and PV on a relevant isentrope. For these two fields, the absolute value of the derivative of the interpolated fields along the direction normal to the jet core is also studied.

When compositing anomaly jet-centred fields, we can compute the p-values of the result using bootstrapping. We correct the false discovery rate (FDR) of these p-values using the Benjamini-Hochberg procedure, also named FDR correction (Benjamini and Hochberg, 1995; Wilks, 2016).

3 Results

3.1 Two case studies

We illustrate representative synoptic situations during persistent jet episodes and associated impacts for two case study periods. The first one occurred from 7 August 2003 06:00 UTC to 13 August 2003 00:00 UTC, at the height the 2003 heat wave in France (see e.g. García-Herrera et al., 2010, for a review of the episode). It was a persistent episode of the STJ according to our definition. Large positive temperature ($+8\,\mathrm{K}$) and geopotential height anomalies ($+200\,\mathrm{m}$) were already present over most of

https://doi.org/10.5194/egusphere-2026-1045
Preprint. Discussion started: 10 March 2026

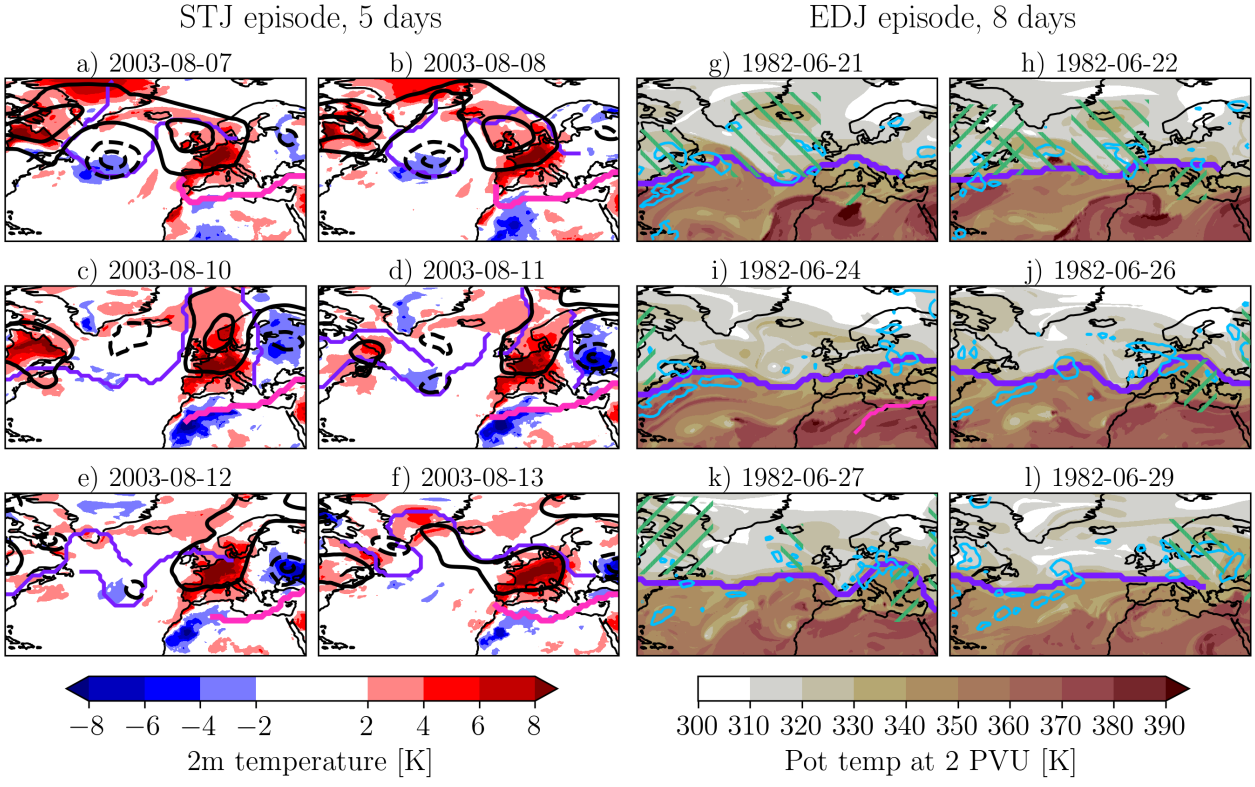

Figure 2. Case studies: a persistent episode of the STJ (a-f) and one of the EDJ (g-l), illustrated with snapshots of relevant spatial variables spanning the length of the event. Thick pink lines: detected STJ cores. Thick purple lines: detected EDJ core. Panels a-f: shading 2 m temperature anomalies, black contours geopotential height anomalies with levels every 100 m except 0 m, dashed contours represent negative levels. Panels g-l: shading potential temperature on the 2 PVU isosurface, cyan contour precipitation above 15 mm. Cyclonic- or anticyclonically oriented green hatching cyclonic or anticyclonic PV overturnings.

western Europe by 4 August (Figure 2a) and remained until the end of the episode (Figure 2b-f). By definition, the STJ core's position changed little over time. The STJ was located about three degrees further south than its August climatological position. During this episode, the EDJ was very wavy and variable over the North Atlantic and is positioned north of the anticyclone over Europe, at a larger than climatological meridional distance from the STJ. The STJ was therefore not interacting with the transient eddies of the EDJ and remained stationary.

The second case study presents a persistent episode of the EDJ from 20 June 1982 18:00 UTC to 29 June 00:00 UTC. The episode started with an unusually zonal and south-shifted EDJ (Figure 2g), CWB north of the jet created a small trough to the west of the UK (Figure 2h) that slowly moved eastward over the next days. A ridge formed towards the end of the episode, co-occurring with a heat wave over Italy (Ap, 1982). Heavy precipitation was falling over the Gulf Stream region and over the British Isles throughout most the episode (Figure 2g-l), and flooding was reported in the United Kingdom towards the end of

https://doi.org/10.5194/egusphere-2026-1045
Preprint. Discussion started: 10 March 2026

the episode (Times, 1982). We hypothesise that the RWB activity on either side of the jet helped maintain the jets eastward extension and CWB on the poleward flank of the jet near the beginning of the episode (Figure 2g-h) maintained the jet's equatorward shift. There was also a contribution from latent heating to the across-jet temperature gradient on the equatorward flank of the jet at its entrance region. Furthermore, while the RWB was strong enough to maintain the jet for a long time, it was not strong enough or located close enough to the jet to imprint large deformations to its core. The STJ was too weak to be detected by our algorithm (with the exception of 24 June).

Selecting periods only by jet persistence has highlighted two interesting situations where jet dynamics and extreme events were connected. We now move to a study of a set of 30 of them to establish more systematic conclusions.

3.2 Jet properties before and during persistent episodes

Shortly before persistent episodes the STJ is located equatorward of its usual position, on higher isentropes, and it is faster during persistent episodes (Figures 3a, b and c). The STJ is also slightly more tilted (Figure 3d) and less wavy according to the metric developed in Röthlisberger et al. (2016, hereafter R16) (Figure 3e), and shows less variance in jet speed during its persistent episodes compared to the summer average values (Figure 3f). The latitude signal can partially be explained by the significant portion ($\sim 50\%$) of persistent STJ episodes that take place in the early or late summer, as shown in figure 1. In early summer the STJ is still at its cold season position (Banderier et al., 2025). It is interesting to see that even though our metric is only affected by geometric and spatial persistence, we also found a jet that is persistent in its average wind speed. During persistent episodes of the STJ, the EDJ also departs from its mean summer state. The EDJ is shifted poleward, located on lower isentropes and more poleward tilted (Figure 3a, b and c). The unusually large latitudinal distance between the EDJ and the STJ might be related to a blocking anticyclone, a hypothesis that we explore further in the following sections. Restricting to the 16 episodes happening outside of the 10 first or last days of the selected period (not shown) reveals that all the signals discussed above still hold and thus are not a result of the seasonal distribution of events but rather a property of persistent jets, with the exception of STJ jet speed which, for this subset of episodes, is at climatological level on average.

The EDJ is located further equatorward, on higher isentropes, and is stronger and less wavy throughout its persistent episodes (Figure 3g, h, i and k), and the wind speed variability is reduced (Figure 3l). The STJ is shifted equatorward and weaker during persistent episodes of the EDJ. The EDJ episodes are evenly distributed throughout summer (Figure 1a), therefore these signals cannot be explained by seasonal variations in the jet properties.

3.3 Sensible weather during persistent episodes of the jet

Since the literature reports strong links between jet stationarity and extreme precipitation or heat events, we study the surface conditions during persistent episodes of both jets using composite anomaly maps. A widespread positive $2\,\mathrm{m}$ temperature anomaly over western, central and northern Europe as well as the British Isles can be observed during persistent STJ episodes in Figure 4a. The temperature anomaly is accompanied by a positive geopotential height anomaly, which is in line with the northward shift, positive tilt and weakening of the EDJ during persistent episodes of the STJ and hints at an interplay between the jets that might be mediated by blocking. Figure 4c shows a widespread dry anomaly in regions of Europe mostly overlapping

https://doi.org/10.5194/egusphere-2026-1045
Preprint. Discussion started: 10 March 2026

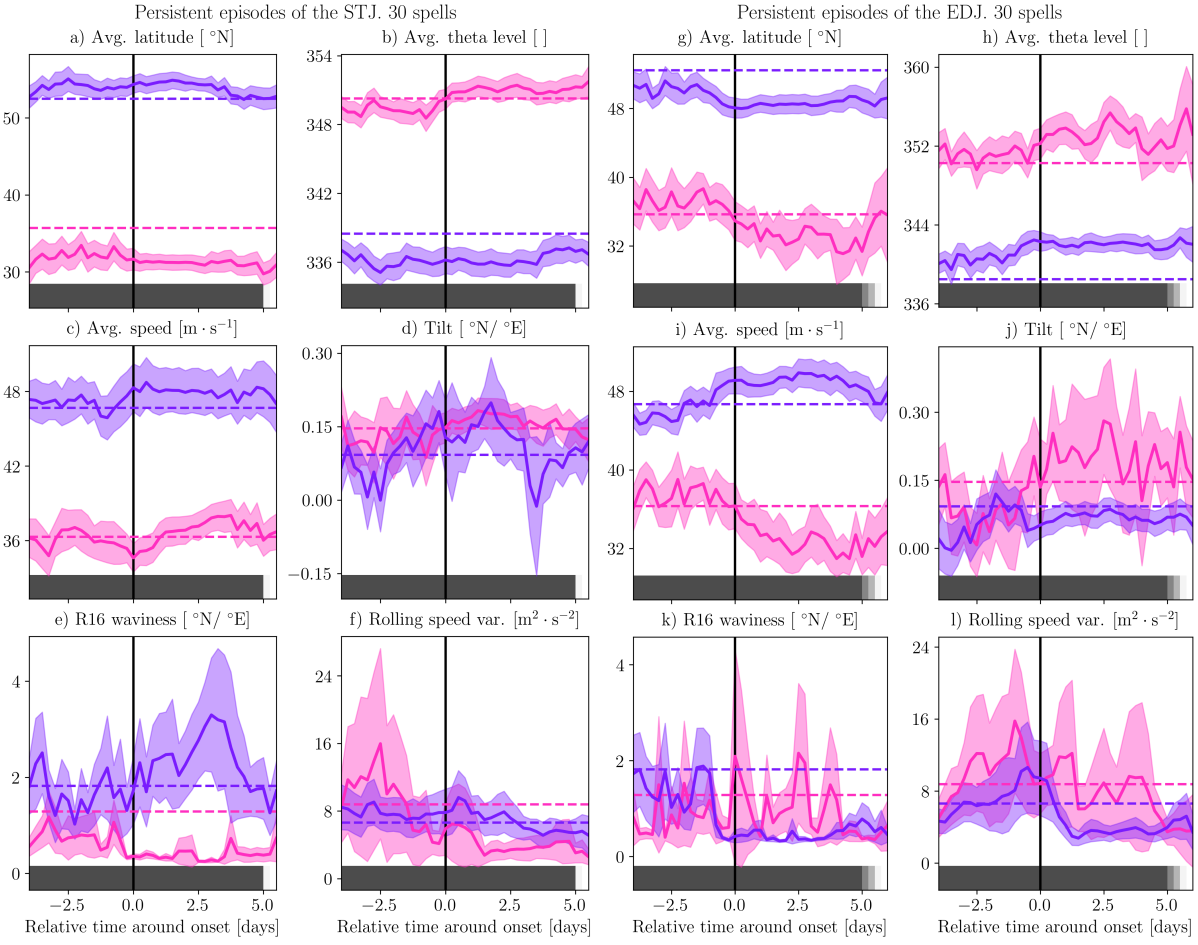

Figure 3. Jet stream properties composited around the onset of a persistent episode of the STJ (panels a through f) and of the EDJ (panels g through l). The grey shading indicates how many episodes are still ongoing relative to the total number of episodes. The shaded areas around the lines show the confidence intervals for the aggregations (mean or variance) at the 90th percentile confidence level. The dashed horizontal lines show the climatological values for the variable over the extended summer period.

with the hot anomaly. The north-western coast of Norway and the Black Sea are significantly highlighted as precipitation hot spots during persistent episodes of the STJ, while the British Isles, as well as central and northern Europe are drier throughout the episodes. No dry anomaly is significant, however.

For persistent episodes of the EDJ, Figures 4b and d reveal cold and wet conditions across the British Isles, Scandinavia and the Baltic region, accompanied by a weak trough. The cold anomalies are however not significant. Southern and western Europe experiences hot and dry conditions during this period. The warm anomalies are significant but not the dry anomalies.

https://doi.org/10.5194/egusphere-2026-1045
Preprint. Discussion started: 10 March 2026

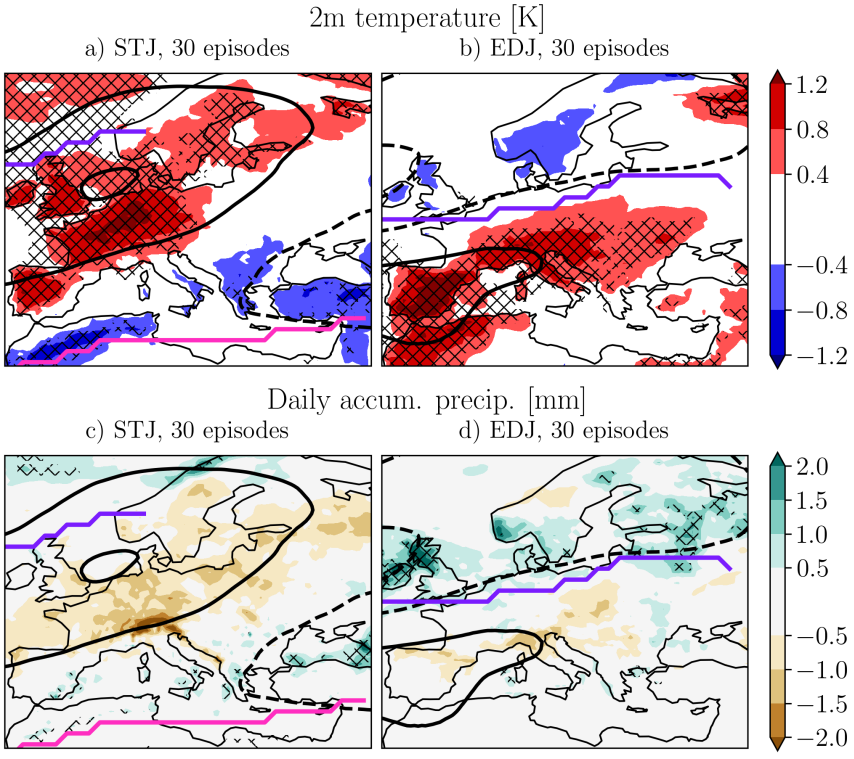

Figure 4. Atmospheric temperature at two metres (top row) and daily accumulated precipitation (bottom row) in Europe for the first three days after the onset of persistent episodes of the STJ (left) and of the EDJ (right), in filled contours. Crosses indicates anomalies significant at the 95% confidence level and using FDR correction. Black contours indicate composite geopotential height anomalies, full lines for positive and dashed lines for negative levels, starting at $-60\,\mathrm{m}$ and ending at $+60\,\mathrm{m}$ by increments of $40\,\mathrm{m}$. Representative jet positions are shown by thick lines computed by detecting jets in the composited wind field (not shown but constructed identically to the other fields).

For an overview of these results over the full duration of the episodes and up to four days before their onsets, we regionalise the temperature and precipitations anomalies shown in figure 4 using the six European heat wave regions defined by Pappert et al. (2025) (see Figure 5e).

Four regions to the North, East and South of Europe already experience positive temperature anomalies of between $0.5\,°\mathrm{C}$ and $1\,°\mathrm{C}$ four days before the onset of persistent episodes of the STJ (Figure 5a). These anomalies decrease to zero within the first five days of the episodes. Western Europe and the Iberian Peninsula experience increasing temperature anomalies from the day before the onset up to six days into the episodes. At the same time, only western Europe experiences notable precipitation anomalies, with increasingly dry anomalies throughout the lengths of the episodes.

Four days before onset of the EDJ episodes, four regions experience moderate negative temperature anomalies. For western and northern Europe, these reach a level close to zero early into the episodes, while eastern and southern Europe, including Iberia, experience warmer than usual temperature persisting up to eight days into the episodes (Figure 5b). Iberia experiences

https://doi.org/10.5194/egusphere-2026-1045
Preprint. Discussion started: 10 March 2026

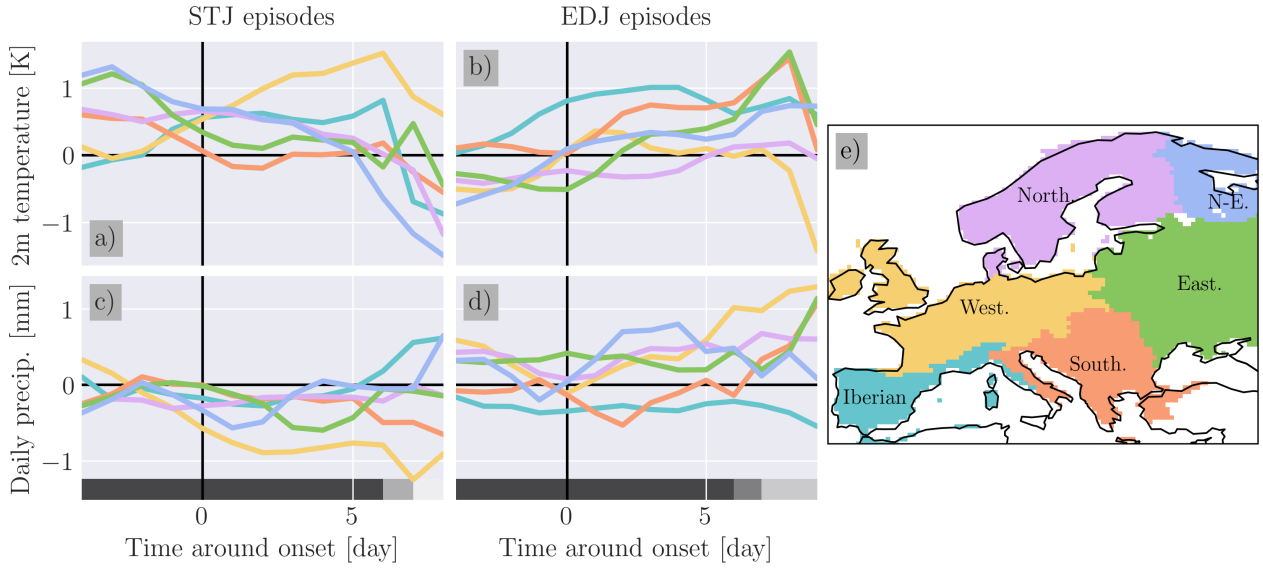

Figure 5. regionalised temperature (top row) and precipitation (bottom row) anomalies before and during persistent episodes of the STJ (left) and of the EDJ (right). Panel e: Heat wave regions from Pappert et al. (2025).

dry conditions, while the western, northern, eastern and north-eastern regions are moderately wetter than usual (Figure 5d). It is interesting to note that these regions were defined using heat wave temporal coherence and yet match quite well the spatial features of the precipitation anomalies in our case.

Beyond the overall weak signals in the mean anomalies, we want to assess if the persistent episodes of the jets can lead to - or could be triggered by - extreme weather events. To that end, we use the regionalised temperature and precipitation time series introduced in figure 5 to find hot, wet, or dry spells. Respectively, these are defined as at least three days with temperature above its JJAS 95th percentile, at least three days with precipitation above its JJAS 95th percentile, and at least three days with precipitation under its JJAS 5th percentile. These simple definitions are close to ones used in recent literature (e.g. Wang et al., 2025; Ali et al., 2021) and yield approximately the same number of extreme events each per region.

In table 1, the odds ratio of extreme events of each type that take place during persistent episodes of either jet, against those that take place outside of persistent episodes, are reported. This shows that hot spells are positively associated with persistent episodes of the STJ in three regions (Iberia, West and North), as are dry spells in four regions (all except North and N-E). Conversely, wet spells in two regions (West and East) are positively associated with persistent episodes of the EDJ. Hot and wet spells of region East are both positively associated with EDJ episodes, suggesting a large variability in the synoptic situations during EDJ episodes.

https://doi.org/10.5194/egusphere-2026-1045
Preprint. Discussion started: 10 March 2026

Table 1. Odds ratio between the persistent episodes of the STJ or the EDJ and regional extreme events. Values significantly different from 1 at the 95% confidence level are reported in bold text.

Event type, **Jet**	**Iberian**	**West.**	**South.**	**North.**	**East.**	**N-E.**
Hot spell, **STJ**	**3.3**	**2.7**	0.5	**2.0**	1.2	0.9
Hot spell, **EDJ**	0.0	1.2	0.0	1.4	**2.0**	1.1
Dry spell, **STJ**	**2.5**	**5.7**	**2.4**	0.8	**2.1**	1.1
Dry spell, **EDJ**	0.0	0.0	0.6	0.0	**0.1**	0.0
Wet spell, **STJ**	0.5	0.4	0.6	0.4	1.0	0.0
Wet spell, **EDJ**	1.3	**2.7**	0.0	1.1	**2.4**	1.1

3.4 State of the atmosphere around the jets

In this section, we use the jet-relative coordinate composites described in section 2.4 to study the state of the atmosphere in the region directly surrounding the STJ and the EDJ during the first three days of their persistent episodes. The summer means of the daily climatologies of jet-centred fields are also shown to support the interpretation of the anomalies during persistent episodes.

During persistent episodes of the STJ a large and widespread positive upper-level temperature anomaly is located on the equatorward flank of the STJ (Figure 6b), co-located with a negative PV anomaly on the 350 K isentrope (Figure 6f), consistent with the mean equatorward shift of the jet (Figure 3a). These broad anomalies strengthen the cross-jet potential temperature gradient (Figure 6d), in accordance with the intensification of the STJ during its persistent episodes (Figure 3c). The anomalies in potential temperature gradient are however mostly not significant.

We note that the potential temperature gradient, both the climatology and the anomaly during persistent episodes, is not centred on the jet but instead shows a slight poleward shift. This bias is a technical artifact coming from two different sources, the preprocessing of the wind speed field before applying the jet detection, and the slight misalignment between the chosen isosurface and the surface on which the jets were detected. An in-depth analysis of this bias, and why none of the potential solutions could be applied, can be found in the Appendix to this article.

The 250 hPa EKE is weaker all around the STJ, especially on its cold flank. This is in line with the poleward shift of the EDJ during the STJ episodes, and another sign of the reduced waviness and speed variability observed on Figure 3e and f. The surface is anomalously warm all around the horizontal position of the STJ (Figure 6i), consistent with the equatorward shift of the jet. Precipitation is reduced around the core and on its cold flank, while increased precipitation is present from 1×10^6 to 2×10^6 m equatorward of the jet entrance (Figure 6l), suggesting enhanced convective activity in the (sub-)tropics, although this result is not statistically significant. Finally, the anticyclonic RWB frequency is increased on the cold flank of the entrance region of the STJ and significantly decreased on the warm flank of the jet (Figure 6n), while cyclonic RWB is insignificantly reduced all around the jet.

https://doi.org/10.5194/egusphere-2026-1045
Preprint. Discussion started: 10 March 2026

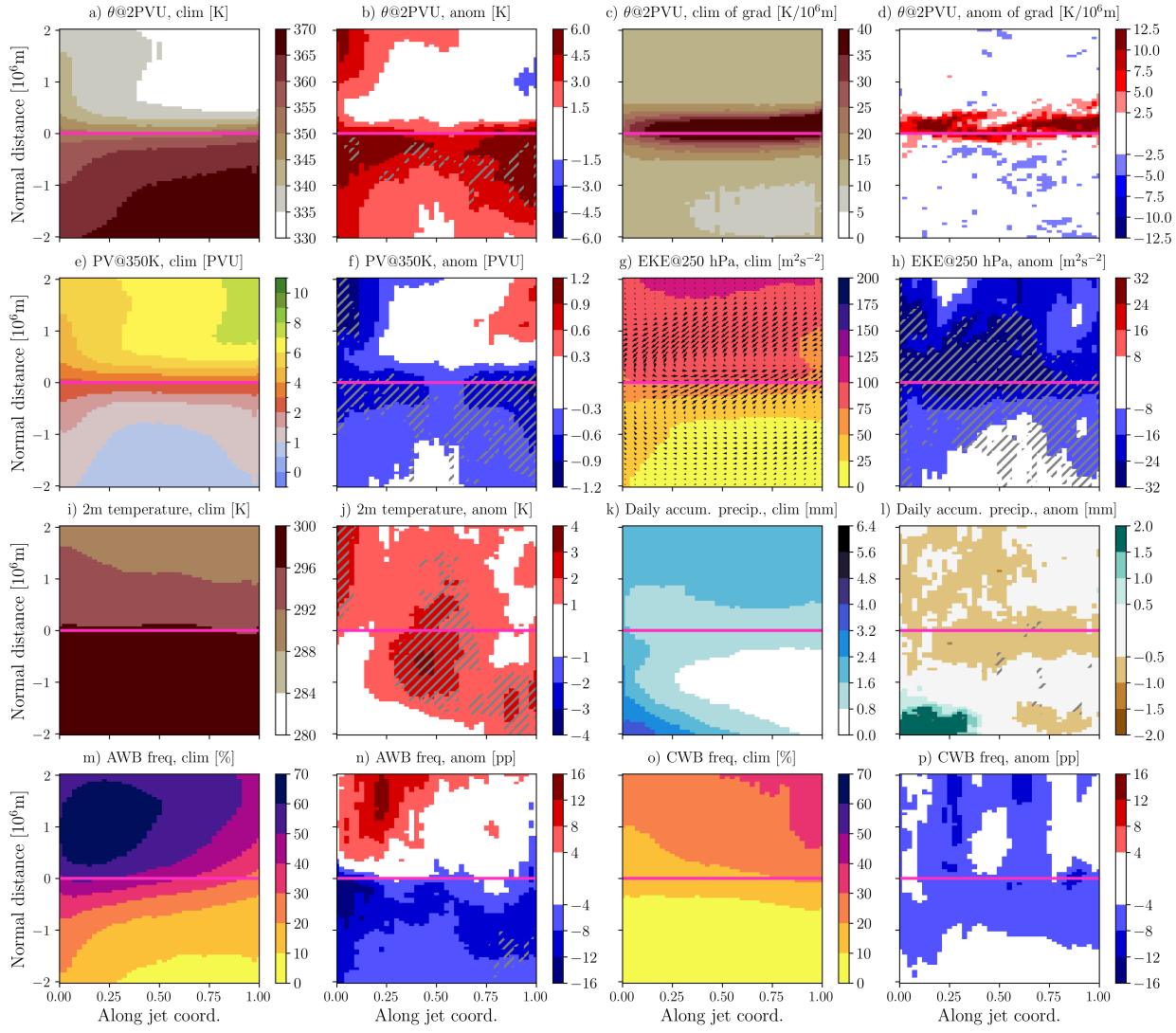

Figure 6. Seven atmospheric, surface or column variables interpolated around the STJ core, composited up to three days after the onsets of every persistent episode of the STJ, relative to a daily climatology of such interpolated fields. For potential temperature, the absolute value of the derivative in the direction normal to the jet is provided as well. The JJAS mean daily climatologies are shown on the first and third columns (panels a, c, e, g, i, k, m and o), while the anomalies are shown in the second and fourth column (panels b, d, f, h, j, l, n and p) with grey hatching indicating pixels whose value has a statistically insignificant difference to the climatology, using FDR correction. Panels a and b: potential temperature on the 2 PVUsurface. Panels c and d: absolute value of the cross-jet derivative of potential temperature on the 2 PVUsurface. Panels e and f: potential vorticity on the 350 K isentrope. Panels g and h: Eddy kinetic energy at 250 hPa. On Panel g, the arrows represent horizontal eddy velocities. Panels i and j: Atmospheric temperature at 2 m. Panels k and l: Daily accumulated precipitation. Panels m and n: AWB frequency. Panels o and p: CWB frequency.

https://doi.org/10.5194/egusphere-2026-1045
Preprint. Discussion started: 10 March 2026

During persistent episodes of the EDJ significant positive upper-level temperature anomalies are present on the warm flank of the EDJ (Figure 7b), which results in a stronger than average potential temperature gradient on the poleward flank of the jet (Figure 7d), albeit weaker than the same result for the STJ, and also mostly insignificant. The strengthening of the cross-jet temperature gradient is in line with the intensification of the EDJ during its persistent episodes via the thermal wind balance. Another region of enhanced temperature gradient 15° south of the EDJ core 7d) corresponds to the preferred STJ position during these episodes (see Figure 3g).

On the $330\,\mathrm{K}$ isentrope, a negative PV anomaly is visible on the warm flank of the jet and along its core up to $6 \times 10^5\,\mathrm{m}$ into its cold flank (Figure 7f). On the cold flank, four roughly equidistant regions of positive PV anomalies are visible. We interpret this pattern as high spatial coherence between persistent EDJs of various episodes, specifically as four preferred positions of their individual troughs. Likewise, EKE is decreased all around the jet except in four small regions close to the core on its cold flank (Figure 7h), Rossby wave breaking of either type is decreased all around the jet, and the AWB frequency anomalies also present the same four-region pattern. With the positive PV anomalies in these regions, the EKE anomalies are expected to come from more cyclonic eddies. All RWB results are however not statistically significant.

The surface temperature is overall warmer around the position of the EDJ (Figure 7j), in a pattern similar to that of the upper-level potential temperature (Figure 7b). Precipitation show mostly statistically insignificant wet anomalies on either flank of the jet, close to the core, following again the four-region pattern (Figure 7l), and dry anomalies further equatorward.

3.5 Individual spells

The objective of this section is to go beyond the mean across persistent episodes and study the state of previously discussed variables participating in the onset and maintenance of each individual episode. To that effect, we select a subset of most relevant two-dimensional fields (variables on various isosurfaces) interpolated on the jet-centred plane, aggregate their values over a region of that plane, and average the result over the first three days of the episode, or over the last three days before the onset. We add to the fields presented in the previous section the most frequent North Atlantic summer weather regime (Cassou et al., 2005; Grams et al., 2017), and selected jet properties. We present either absolute values or anomalies with respect to a summer mean climatology when deemed most relevant for ease of interpretation. The aggregations regions are "warm flank" ($-1 \times 10^6\,\mathrm{m} \leq n \leq 0$), the "cold flank" ($1 \times 10^6\,\mathrm{m} \geq n \geq 0$) or the "core" ($-1 \times 10^6\,\mathrm{m} \leq n \leq 1 \times 10^6\,\mathrm{m}$) of the jet-centred plane, spanned by the coordinates τ along the jet and n normal to it. Note that they are more limited than the extent of the composites of figures 6 and 7. Two special regions will be used for precipitation, which show more local signals. Far in the tropics on the warm flank of the STJ core, labelled "far" ($-2 \times 10^6\,\mathrm{m} \leq n \leq -1 \times 10^6\,\mathrm{m}$), and one limited to the entrance region of the EDJ, labelled "entrance" ($0 \leq \tau < 0.33$).

For fields representing wave breaking events, the number reported (in $\%$) is to be understood as the mean fraction of the region's area occupied by the event. Two additional columns on the right represent the mean across all persistent episodes, and the mean over the extended summer daily climatology of the row's quantity. Finally, we group the episodes based on the presence or absence of relevant mechanisms for persistence, which will be different for the STJ and the EDJ and will be detailed in the following subsections.

https://doi.org/10.5194/egusphere-2026-1045
Preprint. Discussion started: 10 March 2026

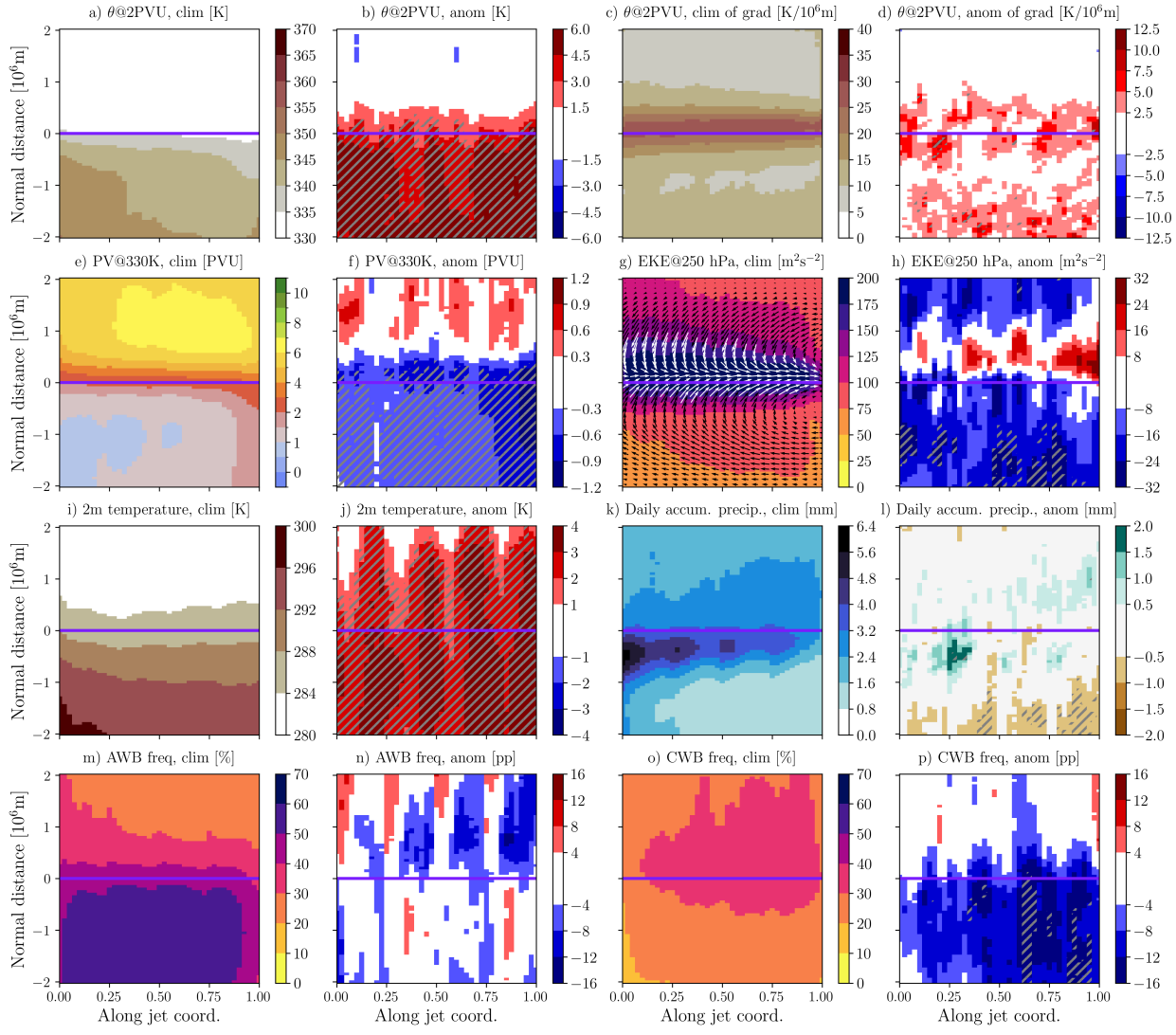

Figure 7. Same as figure 6, but for 30 persistent episodes of the EDJ. Potential vorticity is shown on the 330K isentrope on panels e and f. The colours of the arrows of panel g are only different for contrast reasons.

3.5.1 STJ

Fourteen of the thirty STJ episodes happen mainly within the first or last ten days of the considered period (labelled in orange or magenta on Figure 8) and those are always accompanied by an equatorward anomaly in jet latitude, relative to the expected position at that time of year. This is indicative of the jet staying at its cold season position (Banderier et al., 2025) later in the summer than in most years, and we can surmise that the STJ is more persistent at this position, where it is most influenced by tropical convection and not by extratropical eddies, than at its midsummer position (Martius and Wernli, 2012).

https://doi.org/10.5194/egusphere-2026-1045
Preprint. Discussion started: 10 March 2026

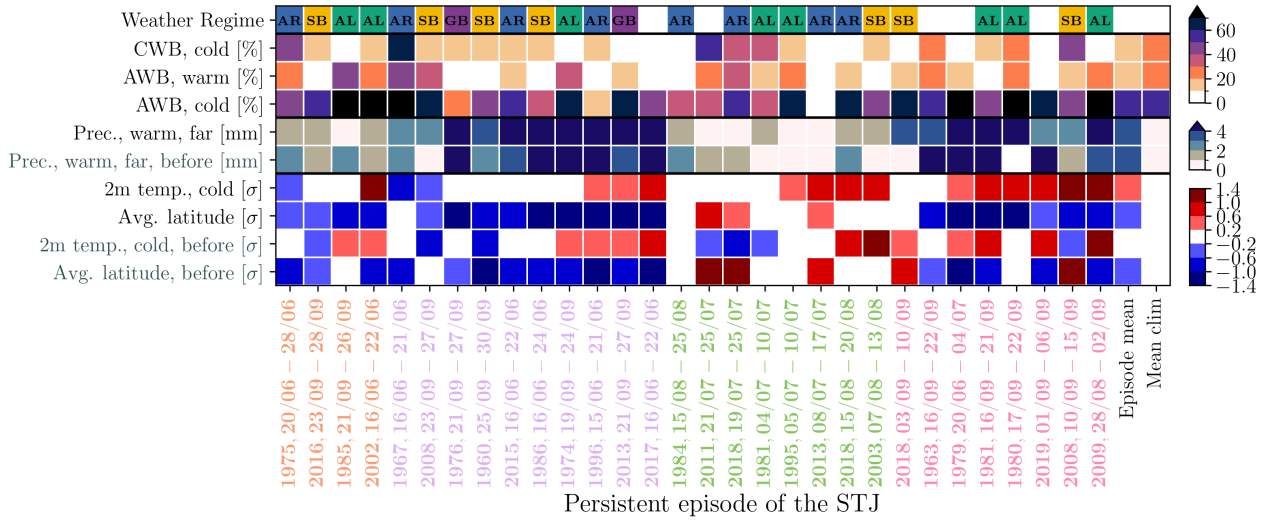

Figure 8. Summary of relevant quantities averaged over a region around the jet in the natural coordinates plane, and over the first three days of the episode. The episode label colours represent a grouping of episode based on mechanisms detailed in the main text. Orange: early or late summer (ELS) and climatological tropical precipitation (TP). Magenta: ELS and enhanced TP. Green: Midsummer and climatological TP. Pink: Midsummer and enhanced TP. Within each group, the episodes are sorted by cold flank 2 m temperature. The second-to-rightmost column reports the mean over all episodes, and the rightmost columns reports the mean of the summer daily climatology. Colours of the weather regimes and of the text in the corresponding boxes are arbitrary.

The tropical precipitation is at least twice as intense than climatology for 18 episodes out of 30. This represents 10 out of 14 early or late summer episodes (in magenta on Figure 8) and 8 out of 16 midsummer episodes (in pink). These latter episodes all feature an unseasonally equatorward jet except one. This means the precipitation sampled for the magenta episodes are further South than the green episodes, which could be the cause for enhanced cold flank precipitation and not actual increases in tropical conditions. We note that the wet signal is typically already present at the onset of the episode.

All weather regimes are represented in similar proportions, but also within each group, indicating that there is no distinction between the early or late summer and midsummer episodes, except that no midsummer episode co-occur with the Greenland Blocking regime. This latter statement is not statistically significant if one models weather regimes using a categorical distribution with climatological frequencies of each weather regime.

Cold flank CWB and warm flank AWB are both less frequent during persistent episodes and are overall very rare, even when restricting to only midsummer episodes (green and pink), compared to summer climatology shown in the rightmost column. No episode shows an above climatological area fraction of warm flank AWB, and only five show an above average cold flank CWB, three of them in midsummer.

In agreement with the mean signal in Figure 6n, cold flank AWB is more frequent than on average and more widespread than the climatology for 13 out of 30 episodes. The large cold flank AWBs are often accompanied by positive temperature

https://doi.org/10.5194/egusphere-2026-1045
Preprint. Discussion started: 10 March 2026

anomalies. These cold flank warm temperature anomalies are present for fourteen episodes out of 30, and only two are not accompanied by enhanced cold flank AWB. Warm anomalies precede the onset of the persistent episode 10 times out of 14, which is in line with the pre-existing temperature anomalies in many regions visible on figure 5a.

3.5.2 EDJ

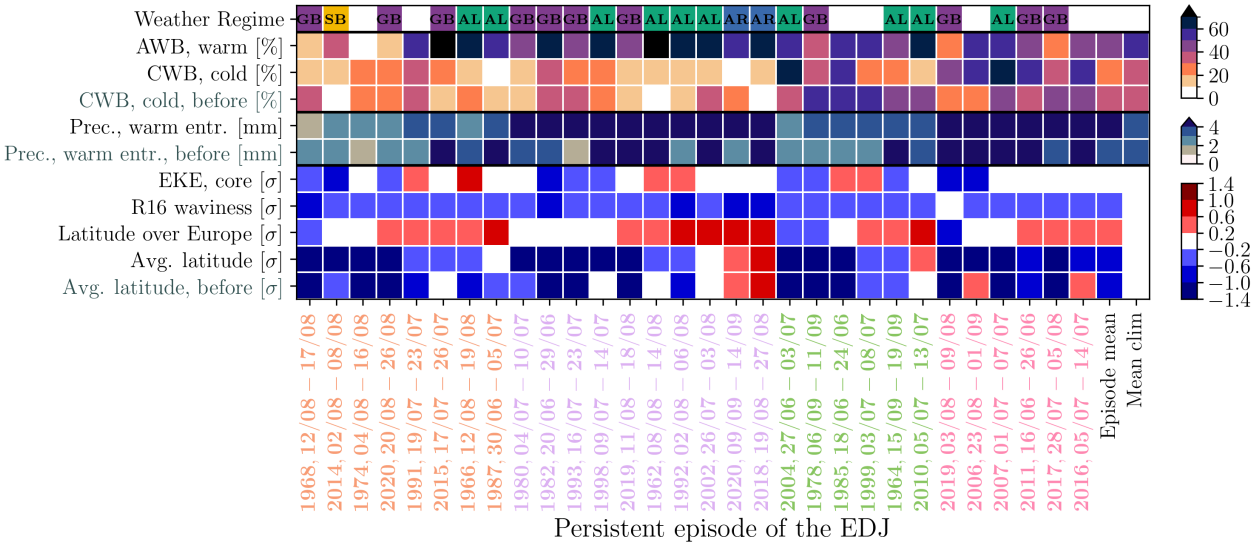

Figure 9. Same as figure 8, but for episodes of the EDJ. A similar grouping of episode is applied here, based on warm flank precipitation and cold flank CWB, before or during the episode, compared to climatology. Orange: lower-lower, magenta: higher-lower, green: lower-higher, pink: higher-higher. In each group, the episodes are sorted by increasing average latitude over Europe.

Averaged over all episodes, cold flank CWB is less widespread than climatology by 10 percentage points. There are however 12 episodes for which it is as widespread or more than climatology, either during or before the episode. The subset of these episodes with enhanced warm flank precipitation (in pink in Figure 9) shows more CWB during the episode than before, while the subset without enhanced warm flank precipitation (in green) shows more CWB before the episode. The green and pink episodes also correspond to less widespread warm flank AWB than the remaining episodes. The average jet latitude shows a similar proportion of negative anomalies with or without enhanced cold flank CWB, before or during the episode.

On the warm flank and in the entrance region of the EDJ, precipitation is more intense than climatology during 16 episodes (in magenta or pink in Figure 9). The signal is present before the onset of the episode 14 times out of 16.

The EDJ episodes co-occur predominantly with the Atlantic Low or the Greenland Blocking weather regimes, 11 and 10 times, respectively, out of 30 total episodes, with only two episodes co-occurring with the Atlantic Ridge regime and only one with the Scandinavian Blocking regime, the rest being unassigned (Figure 9). The two most represented regimes correspond to a low pressure system over the Euro-Atlantic sector. It is centred above the British Isles in the case of Greenland Blocking, and

https://doi.org/10.5194/egusphere-2026-1045
Preprint. Discussion started: 10 March 2026

over the central North Atlantic in the case of the Atlantic Low regime (Cassou et al., 2005). One can expect an equatorward shifted jet during these regimes, which we observe in all but five EDJ episodes. We note that most of the time this equatorward shift was already present before the onset of the episodes. The Atlantic Low regime is also associated with a weak high pressure system over western Europe, where we expect the jet to shift poleward locally because of it. Accordingly, persistent episodes associated with this regime show positive anomalies in the "Latitude over Europe", which measures the average of jet point latitudes for longitudes eastward of $10°$W, for the persistent episodes.

The jet is less wavy than usual during all of its persistent episodes according to the R16 metric. Around the jet's core, upper-level EKE is reduced for 11 episodes out of 30 and increased six times, and the increase is limited to the jet's cold flank in the mean according to Figure 7h. This EKE decrease is neither linked to a specific weather regime nor to significantly less likely CWB, but jet core EKE is positively correlated with the the jet's latitude over Europe ($\rho = 0.54$).

4 Discussion

Averaged over all their thirty most persistent episodes, both jets are located further equatorward during persistent episodes and on a warmer isentrope. They are stronger and less wavy compared to their mean summer state. Around the jets, the potential temperature gradient on the $2\,\mathrm{PVU}$ surface is intensified, and so is the PV gradient on the relevant isentrope ($330\,\mathrm{K}$ for the EDJ, $350\,\mathrm{K}$ for the STJ; see Appendix). These stronger gradients are consistent with higher wind speeds according to the thermal wind balance and the PV gradient – lateral wind shear relationship (e.g. Davies, 1981). The enhanced PV gradient is also expected to increase the waveguiding ability of the jet during its persistent episodes (Martius et al., 2010; Wirth, 2020). Surface temperature around the core of the jet is increased on either flank of the jet, both as a consequence of the equatorward shifts sampling higher temperatures and from significant positive temperature anomalies in different regions of Europe during persistent episodes. The last common feature of STJ and EDJ persistent episode is the overall decrease of eddy activity and RWB around the jet core in the mean.

Persistent episodes of the STJ are not distributed evenly across summer, but are instead most common during the first and last ten days of the study period, and rarest in early August. While the persistence metric is slightly higher on average than that of the EDJ, the episodes are typically shorter; the most common episode length is just under 6 days, while the minimum imposed length is 5 days. We extracted three explanatory mechanisms for the onset and maintenance of persistent STJ episodes.

The simplest mechanism is the jet being in its cold season position at the start or at the end of our study period, further equatorward than its summer mean state, which is uncommon but not exceedingly rare, as it can stay in this position until as late as early July (Banderier et al., 2025). The equatorward shift is weakly linked to Hadley cell seasonality (Dima and Wallace, 2003; Menzel et al., 2019) and, more locally, to the poleward shift of the West African monsoon in late June (e.g. Peyrillé et al., 2016). In its cold season position, the STJ interacts less with extratropical sources of momentum, i.e., eddies, and more with tropical sources (Martius, 2014), yielding less daily variability in latitude, but also in wind speed as figure 3f also showed.

The second mechanism, which can compound with the first, is active deep convection far equatorward of the jet, feeding more momentum of tropical origin to the STJ. As an indicator of this, tropical precipitation was enhanced by a factor ranging

https://doi.org/10.5194/egusphere-2026-1045
Preprint. Discussion started: 10 March 2026

from 2 to 10 for 18 out of 30 episodes (Figure 8), and this wet tropical signal is typically already visible before the onset of these episodes. We also investigated the link to the Madden-Julian Oscillation (MJO), of which phases 1, 2 and 8 are associated with increased convective precipitation over western Africa or the tropical Atlantic Ocean (Madden and Julian, 1972; Zhang, 2005), but no strong link was found.

Finally, a third mechanism, whose imprint is visible in the mean across all episodes, has preceding warm and dry conditions in regions of Europe as well as positive geopotential height anomalies maintaining the STJ equatorward of a large and troposphere-spanning anticyclonic weather system. For this third mechanism especially, the persistence of the STJ seems to be the related to a pre-existing surface temperature anomaly and upper-level anticyclones. The temperature keeps increasing and the precipitation rate keeps decreasing in the most relevant region, western Europe, throughout STJ events, but it is not possible to tell whether the STJ played a role in this intensification, for example by deepening the block via selective absorption of advected anticyclones. This equatorward shift has the same effect as the one discussed in the context of the first mechanism: the STJ interacts more with tropical momentum sources and less with extratropical eddies.

There is enhanced AWB activity on the cold flank of the STJ, i.e., between the STJ and the EDJ, whether the episode happens in early or late summer or in the midsummer. We hypothesise that its impact on the STJ is the same as that of enhanced blocking, that is forcing the jet further equatorward than its climatological position. Depending on the precise location of the cold flank AWB with respect to the STJ core, it may accelerate the jet by enhancing the PV gradient at its core (Hoskins, 2014; Tamarin-Brodsky and Harnik, 2024). Warm flank AWB and cold flank CWB, which may also intensify jets (see e.g. Messori and Caballero, 2015, although in the context of the EDJ), are both less widespread than climatology during STJ episodes, so the weak acceleration of the persistent STJ does not come from this type of wave-breaking.

STJ episodes significantly increase the odds of hot spells in three regions of Europe, and of dry spells in four regions, although the direction in causality is hard to assess since some temperature anomalies are already visible before the onset of the episodes.

In the mean, the EDJ is displaced poleward during persistent episodes of the STJ. In the context of mechanism 1, it is the opposite direction to the one expected from sampling EDJs in early or late summer, since it is supposed to be further equatorward compared to the extended summer mean (Banderier et al., 2025). This poleward shift may best be explained in the context of mechanism 3, with positive geopotential height anomalies accompanying hot and dry anomalies in Europe, which could force both jets on either side of them, as a block would do (Nakamura and Huang, 2018). It could also be a requirement that the EDJ be further away from the STJ and impart fewer synoptic disturbances on it for the STJ to be persistent.

The persistent episodes of the EDJ are evenly spread during summer, so intraseasonal variations do not affect the results. EDJs have an overall lower mean persistence, but the episodes last longer on average, compared to the STJ. The distribution of episode lengths appears bimodal, with a peak at six days and one at eight day, most probably an effect of the low sample size since the length of the persistent episodes does not appear correlated to any of the mechanisms discussed below. We expect eddy activity to be important for the persistence of the EDJ, since at least in winter the eddy feedback is the mechanism that maintains the EDJ. In short, the baroclinic zone associated with the jet and its local increased temperature gradient create transient eddies, which travel away from their source to decay while feeding zonal momentum back into the jet, reinforcing the

https://doi.org/10.5194/egusphere-2026-1045
Preprint. Discussion started: 10 March 2026

temperature gradient, baroclinicity and eddy creation (Hartmann, 2007; Barnes and Hartmann, 2010). We also expect diabatic processes to play an important role in jet persistence (Hoskins and Valdes, 1990).

What we see in the mean across the 30 persistent episodes is an overall decrease in EKE around the core, except in four regions poleward of it core it is enhanced. We identify the four-region pattern in the jet-centred plane as sampling poleward of troughs of the persistent EDJs, that are located at similar preferred locations in the jet-centred plane across episodes to imprint this spatially coherent pattern in the mean. Looking into individual episodes beyond the mean signal reveals that three mechanisms can again be identified to explain EDJ persistence.

The first mechanism is the eddy feedback mentioned in the previous paragraph. It is visible as enhanced cyclonic EKE around the core of the jet in the mean. In a similar fashion, although it is reduced in the mean, CWB is enhanced on the cold flank of the jet either before or during EDJ episodes for twelve episodes. CWB is part of a similar feedback loop with the jet and its latitudinal position, as described by Rivière (2009). CWB forms at the end of the cyclonic baroclinic (LC2-type) life cycle. LC2-type life cycles are more likely to occur when the EDJ is shifted equatorward, and CWBs impart equatorward and eastward momentum fluxes to the jet, accelerating it and maintaining its equatorward shifted position (Simmons and Hoskins, 1978; Hartmann, 2007; Rivière, 2009). LC2 lifecycles are also more persistent than LC1 (Thorncroft et al., 1993; Franzke et al., 2004). From our data, this feedback loop seems to start more often with an unseasonally equatorward shifted jet before the onset of persistent episodes which then have enhanced CWB to maintain them, rather than the opposite. The mechanism of double wave-breaking proposed in several articles (see e.g. Pinto et al., 2014; Messori and Caballero, 2015; Dacre and Pinto, 2020) does not seem to play a major role for our definition of jet persistence, potentially because these events tend to be localized around the East Atlantic and out jet persistence metric takes the whole jet into account.

The second mechanism is more local and concerns the maintenance of the jet over the European continent at a higher than seasonal latitude. In the mean, EDJ episodes co-occur with increased surface temperatures over most of southern Europe and especially the Iberian Peninsula and the temperatures often start rising before the onset of the episodes. The associated positive geopotential height anomalies, part of the Atlantic Low weather regime, maintain the jet over the British Isles and the Baltic Sea. This may also be part of a feedback loop as it is known that jets can help maintain blocks by feeding them anticyclonic eddies (Shutts, 1983; Yamazaki and Itoh, 2013). This block maintenance is enhanced for stronger jets because of the steeper PV gradient and hence waveguiding (Martius et al., 2010; Bukenberger et al., 2023).

Finally, the third mechanism is the increased precipitation on the warm flank and mostly in the entrance region of the jet before and during two thirds of the episodes, and whose signal is clearly visible in the mean but not statistically significant. Via the release of latent heat, this creates and / or strengthens negative PV (positive potential temperature) anomalies at upper-levels above the diabatic heating maximum (e.g. Wernli and Gray, 2024) that give momentum to the jet on its warm flank and reinforce the self-maintenance of the jet (Robinson, 2006; Hartmann, 2007). This PV destruction might play a role in the negative anomaly in cyclonic PV overturnings in the same region, seen in figure 7p, although it is more widespread than the modest area of increased precipitation.

Persistent EJDs are associated with cold and wet conditions at their preferred core locations over the British Isles, the North Sea and the Baltic Sea. Wet spells are significantly more likely during persistent episodes of the EDJ than outside of them in

https://doi.org/10.5194/egusphere-2026-1045
Preprint. Discussion started: 10 March 2026

these regions. Further south of it and linked to the equatorward shift of the STJ over European longitudes, a large portion of southern Europe experiences hot and dry conditions accompanied by a mid-level ridge.

5 Summary and outlook

We investigate the mechanisms behind persistent jet episodes in the Euro-Atlantic sector during the extended summer and quantify the associated surface weather anomalies.

Our study relies on objectively detected jet features extracted from 6-hourly ERA5 wind speed fields and an automatic categorisation of the jet features into subtropical (STJ) or eddy-driven (EDJ) jets. We identify persistent episodes by calculating a distance metric between the jet features at one time step and at the next. The distance metric is applied to the STJ and EDJ separately. We then apply a quantile threshold to the distance metric to extract persistent episodes and then analyse the 30 most persistent episodes in detail (Q1).

Jets that are spatially and geometrically persistent are stronger, shifted equatorward, less wavy, are located on warmer isentropes and show less daily intensity variability compared to the climatologies of these jet properties (Q2). There is also an effect on the other jet, as the EDJ is stronger and further north when the STJ is persistent, and the STJ is weaker and further south when the EDJ is persistent (Q3). Persistent jets are accompanied with enhanced potential temperature gradients around their core, expected with their enhanced intensity, and higher surface temperatures around their core, in line with their equatorward shifts.

While pre-existing warm and dry conditions in western Europe seem to determine the onset of some STJ persistent episodes, we see that these conditions intensify during the episode. Further south, the episodes instead bring cold and wet conditions. The EDJ episodes bring wet and cold conditions in parts of western and eastern Europe, and hot and dry conditions in southern Europe. This influence also translates into significantly increased extreme event odds, compared to non-persistent periods. Hot spells over three regions out of six and dry spells over four for the STJ, and wet spells over two regions for the EDJ (Q4).

The environment around persistent jets also shows typically less eddy activity, indicated by reduced eddy kinetic energy (EKE) and Rossby wave breaking (RWB) in most regions around the STJ and the EDJ. This can be linked to the findings of Coumou et al. (2015), who found that a weaker storm track is associated with more persistent conditions. Two exceptions are a small region of enhanced anticyclonic RWB (AWB) 10 degrees into the warm flank of the STJ, and enhanced EKE in a small band of the warm flank of the EDJ. Finally, the environment around the STJ shows less precipitation when it is being persistent, except in a small band far into the warm flank of the jet in a tropical region. The EDJ sees enhanced precipitation in a narrow region of its warm flank (Q5).

Looking beyond the mean and into individual episodes, we found evidence of three, non-mutually exclusive, mechanisms that may explain persistence of the summer STJ. The first is a late (past 15 June) or early (before 30 September) occurrence of the more stable cold season position of the STJ. The second involves increased tropical convection in the Atlantic basin. Finally, the last one emanates from pre-existing hot and dry conditions over Europe and widespread positive geopotential height anomalies that force the STJ to stay on its equatorward side (Q5).

https://doi.org/10.5194/egusphere-2026-1045
Preprint. Discussion started: 10 March 2026

In the case of the EDJ, we also find evidence of three mechanisms to explain its persistence. The first one involves a positive feedback loop between an equatorward shift of the jet and cold flank CWB, or at least enhanced cyclonic eddy activity, which mutually reinforce each other, maintaining a strong jet (typically more persistent, see Woollings et al., 2018) with an equatorward anomaly. This explanation holds only for a subset of the episodes, while the others instead show a decrease in in CWB and eddy activity. The second mechanism is a positive geopotential height anomaly situated over southern Europe that maintains the jet poleward of it locally, and explains opposite sign latitude anomalies of the jet over Europe compared to over the North Atlantic during several episodes. Since jets are able to reinforce persistent anticyclones with their waveguide ability and the selective absorption mechanism, we can hypothesise that a feedback loop is also at play here. The third mechanism, present for two thirds of the episodes, is an increase in precipitation on the warm flank of the entrance region of the jet, creating negative PV anomalies in this region and therefore reinforcing the jet (Q5, Q6).

The methods used in this work have at least three important limitations. Firstly, the persistence metric is inherently biased in favour of zonal jets. Comparing cases where a deep or a shallow ridge are advected the same eastward distance between two time steps, the case with the deep ridge will show a lower persistence than the case with the shallow one. This is not deeply problematic and fits with the objective of characterising persistence at the local scale, but needs to be kept in mind. Secondly, labelling entire jets as one category and using this information for tracking is the most pragmatic way of working on this problem in the Euro-Atlantic sector, but is not generalisable to sectors where the jets can be hybrid, or can smoothly transition between categories. There, explicit tracking is necessary which might introduce errors but can give interesting information on the evolution of jet type over time, which we cannot do in our framework. Finally, the exact interpretation of eddy kinetic energy in the context of instantaneous jets is not straightforward. Since the eddy velocities were obtained from a 10-day high-pass filter, they relate to a mean flow that would be slowly varying, at the monthly timescale, not to instantaneous jets, which are themselves contributing to the high-frequency signal. There does not seem to be an easy way to separate eddies from instantaneous jet axes, and this relates to the wider problem of mean flow characterisation in tropospheric dynamics (see e.g. Wirth and Polster, 2021).

Even though it is not possible to quantify the effect of global warming in such a short dataset, it is interesting to note that, for example, 15 out of the 30 most persistent episodes of both jets happened in the last 20 years of data out of 64, and that a large proportion of those of the STJ were linked to a hot European surface. Using a large ensemble of model data, ideally with several models, would allow us to gauge how well persistence is represented, and get a much bigger sample size with a longer global warming period to be able to test our hypothesis that jet stream persistence may be enhanced with increasing temperatures.

Code and data availability. ERA5 on single- and pressure levels available from the CDS portal https://cds.climate.copernicus.eu/ (last accessed 10.10.2025). Detected, categorised jets from ERA5, but also timeseries of persistence metric and other useful datasets (Banderier, 2026a), python package with most of the backend code (Banderier, 2026b, including interactive notebooks, all functions used for this work fully documented)

https://doi.org/10.5194/egusphere-2026-1045
Preprint. Discussion started: 10 March 2026

Appendix A: Additional jet-centred composites and exploration of the poleward bias in jet-centred composites

In this appendix, we first display the variables interpolated on the jet-centred plane that were not as relevant for the discussion in the main text, but may still prove interesting to the reader. These include PV gradient anomalies (figures A1d and A2d for the STJ and the EDJ, respectively) on isentropes, which show an alternative view on the already discussed increase in potential temperature gradient on the 2 PVU isosurface. It is also the directly relevant quantity for wave guiding (Martius et al., 2010). The eddy momentum flux convergence is mostly relevant for the EDJ, but the anomalies look too noisy to be easily interpreted on figure A2h. The relative vorticity and meridional wind give us an alternative view on the eddy activity and azonal flow around the jet that does not require selecting a scale. Meridional wind anomalies around the EDJ (Figure A2l) also show the preferred location of troughs and ridges. Finally, the last two quantities demonstrate the alignment problem mentioned in the main text. On the surface where jets are detected, the centroid (green line) and the jet-normal maxima (cyan line) of the wind velocity climatology are consistently several hundred kilometres away from the jet in the positive direction (poleward for zonal jets, Figures A1m and A2m). This bias is also present on the 250 hPa surface (Figures A1o and A2o). The episode-mean anomalies produce less smooth lines, but overall show the same positive bias as the climatology (Figures A1n and p and A2n and p).

To understand where this bias comes from, we show, for a randomly chosen time step within the first year of data, the 0-contours of the horizontal normal wind shear, the first step in our jet detection algorithm. We show this quantity computed directly from the 0.5° resolution wind speed files in pink in figure A3, and computed on the wind speed fields coarsened to 1.5° and smoothed with a window of 7.5° in longitude and latitude, as is done to produce the dataset used in this work, in purple. One can see the abundance of small scale features in the pink contours that forces us to use coarsening and smoothing, as well as the potential for latitudinal bias between the unsmoothed and smoothed lines when the curvature is large such as for the EDJ streak off the coast of Newfoundland. Because of the length scales of anticyclones, which are long and tend to induce an equatorward shift, compared to cyclones, which are shorter and tend to induce a poleward shift, we can surmise that the smoothing will impart an overall equatorward shift in the position of the shear 0-contours. In the jet-centred composites, this will translate in the maximum wind speed being a few hundred kilometres poleward of the jet axis.

Author contributions. OM and TW outlined the study. HB developed the code and performed the study under the supervision of OM and TW. HB wrote the manuscript with contributions and reviews from both co-authors.

Competing interests. At least one of the (co-)authors is a member of the editorial board of Weather and Climate Dynamics. The authors have no other competing interests to declare.

https://doi.org/10.5194/egusphere-2026-1045
Preprint. Discussion started: 10 March 2026

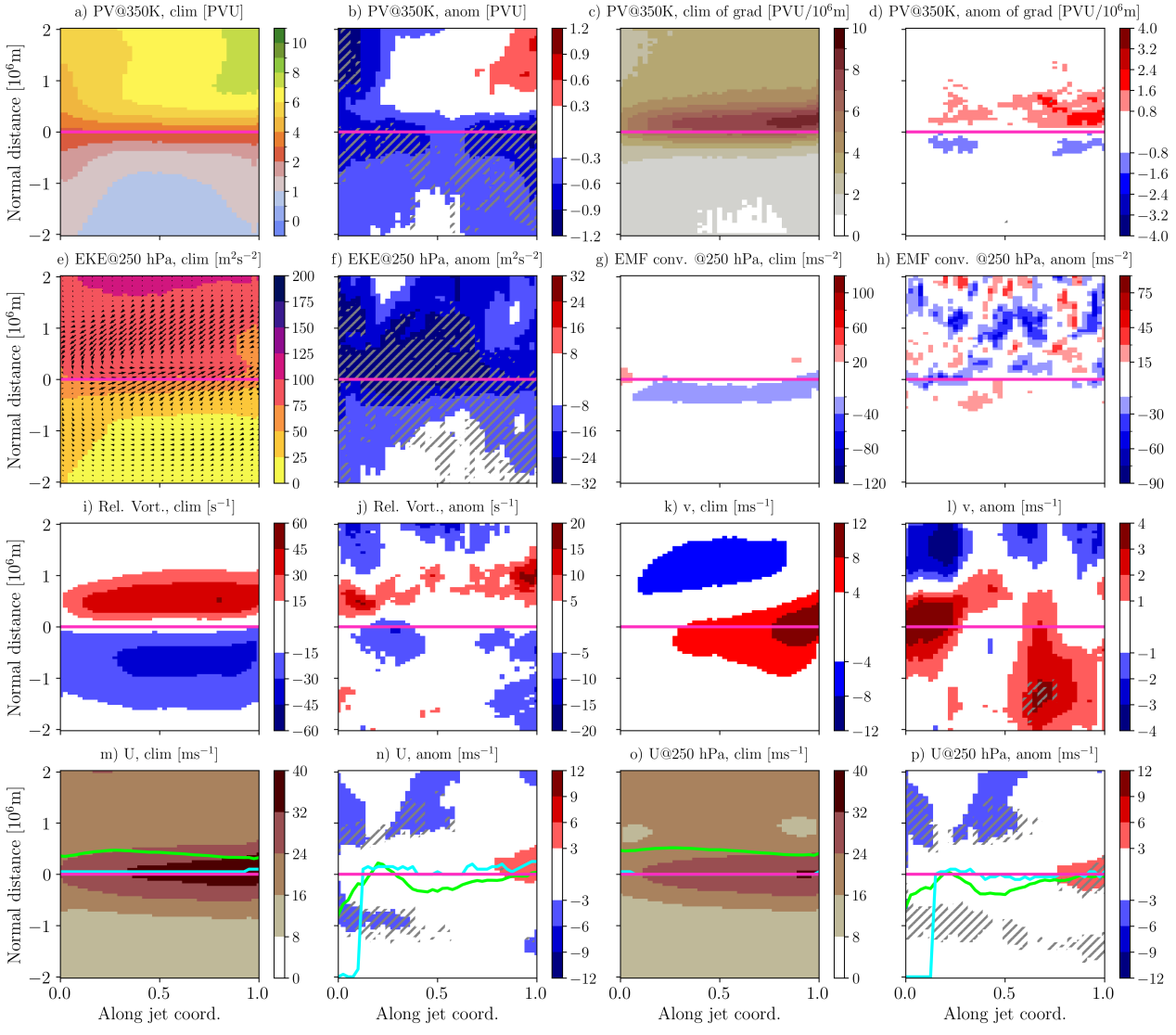

Figure A1. Same as figure 6, but for additional variables not shown in the main text. Panels a and b: potential temperature on the 2 PVUsurface. Panels a and b: potential vorticity on the 350 K isentrope. Panels c and d: absolute value of the cross-jet derivative of potential vorticity on the 350 K isentrope. Panels e and f: Eddy kinetic energy at 250 hPa. On Panel g, the arrows represent horizontal eddy velocities. Panels g and h: Eddy momentum flux convergence at 250 hPa. Panels i and j: relative vorticity on the surface where jets are detected. Panels k and l: meridional wind velocity on the surface where jets are detected. Panels m and n: horizontal wind velocity on the surface where jets are detected. Panels o and p: horizontal wind velocity at 250 hPa.

Acknowledgements. This work was funded by the Swiss National Science Foundation as part of the project "PERSIST-EUROPE" under grant number 200020_207384.

https://doi.org/10.5194/egusphere-2026-1045
Preprint. Discussion started: 10 March 2026

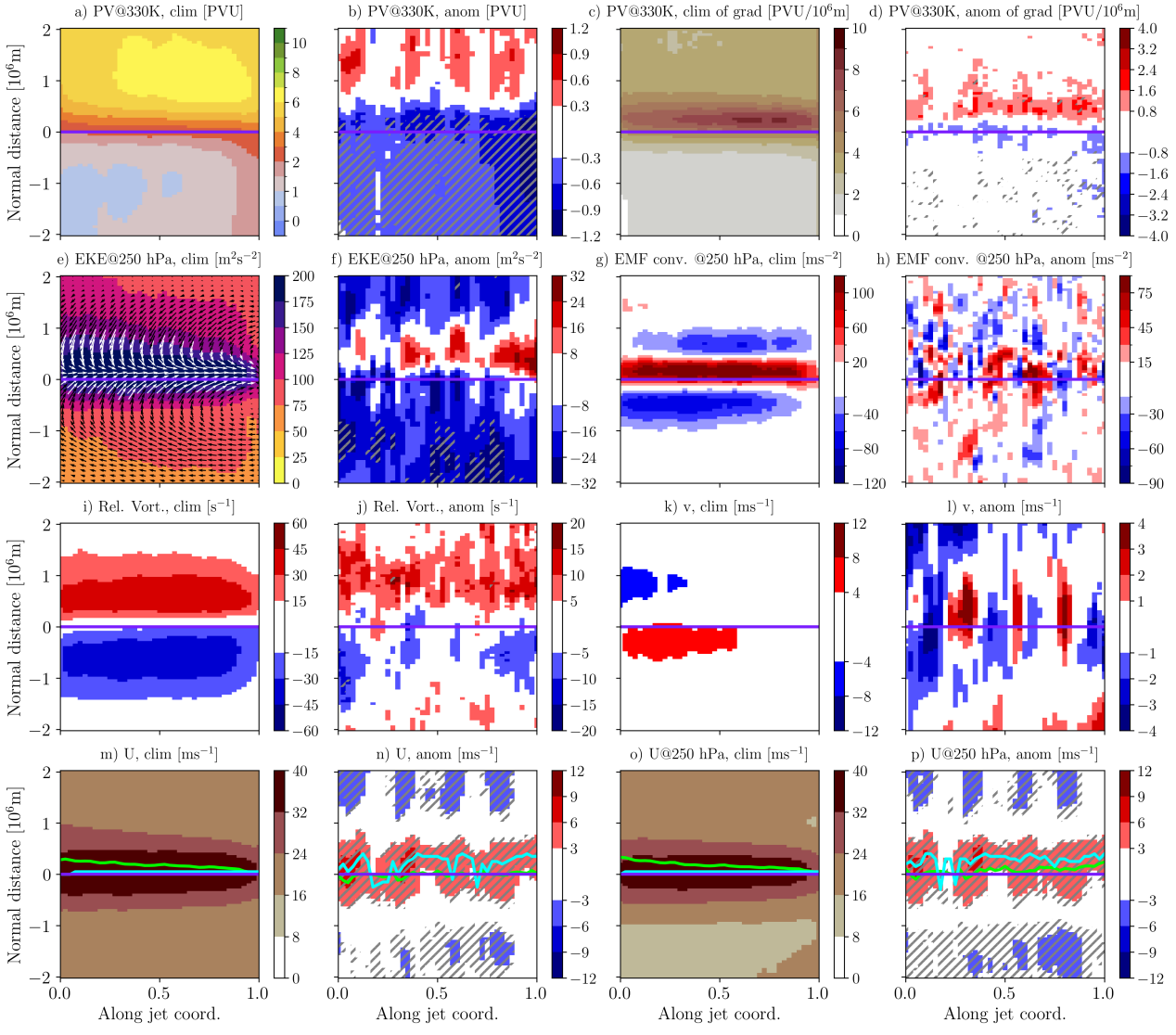

Figure A2. Same as figure A1, but for 30 episodes of the EDJ.

References

Ali, S. M., Martius, O., and Röthlisberger, M.: Recurrent Rossby Wave Packets Modulate the Persistence of Dry and Wet Spells Across the Globe, Geophysical Research Letters, 48, https://doi.org/10.1029/2020GL091452, 2021.

Alt, H. and Godau, M.: Computing the Fréchet Distance Between Two Polygonal Curves, International Journal of Computational Geometry & Applications, https://doi.org/10.1142/S0218195995000064, 2011.

Ap: Heat Wave Sweeps Italy, The New York Times, 1982.

https://doi.org/10.5194/egusphere-2026-1045
Preprint. Discussion started: 10 March 2026

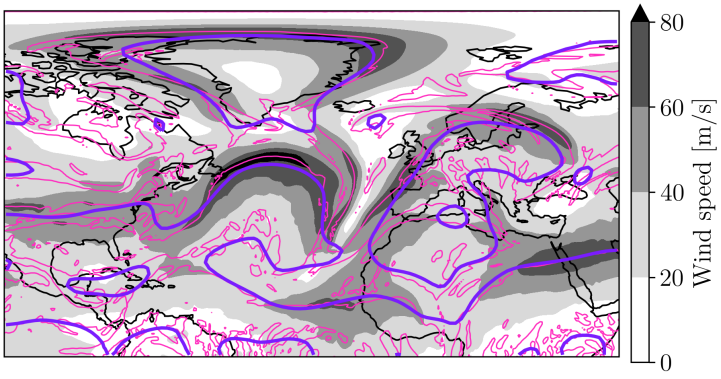

Figure A3. 0-contours of σ, the horizontal normal wind shear. In pink: from raw wind speed. In purple: from wind speed field coarsened and window-smoothed. Shading: raw wind speed.

Auestad, H., Spensberger, C., Marcheggiani, A., Ceppi, P., Spengler, T., and Woollings, T.: Spatio-Temporal Averaging of Jets Obscures the Reinforcement of Baroclinicity by Latent Heating, Weather and Climate Dynamics, 5, 1269–1286, https://doi.org/10.5194/wcd-5-1269-2024, 2024.

Auestad, H., Shibu, A., Ceppi, P., and Woollings, T.: The Latent Heating Feedback on the Mid-Latitude Circulation, Geophysical Research Letters, 52, e2025GL116 437, https://doi.org/10.1029/2025GL116437, 2025.

Banderier, H.: Detected, Categorised and Tracked Jets, Diverse Quantities Interpolated in Jet-Centred Coordinates, https://doi.org/10.5281/zenodo.18471854, 2026a.

Banderier, H.: Jetutils: A Package for Jet Stream Related Utilities, Zenodo, https://doi.org/10.5281/zenodo.18471549, 2026b.

Banderier, H., Tuel, A., Woollings, T., and Martius, O.: Seasonal to Decadal Variability and Persistence Properties of the Euro-Atlantic Jet Streams Characterized by Complementary Approaches, Weather and Climate Dynamics, 6, 715–739, https://doi.org/10.5194/wcd-6-715-2025, 2025.

Barnes, E. A. and Hartmann, D. L.: Dynamical Feedbacks and the Persistence of the NAO, Journal of the Atmospheric Sciences, 67, 851–865, https://doi.org/10.1175/2009JAS3193.1, 2010.

Barnes, E. A. and Hartmann, D. L.: Detection of Rossby Wave Breaking and Its Response to Shifts of the Midlatitude Jet with Climate Change, Journal of Geophysical Research: Atmospheres, 117, https://doi.org/10.1029/2012JD017469, 2012.

Barnes, E. A., Hartmann, D. L., Frierson, D. M. W., and Kidston, J.: Effect of Latitude on the Persistence of Eddy-Driven Jets, Geophysical Research Letters, 37, https://doi.org/10.1029/2010GL043199, 2010.

Bengtsson, L., Hodges, K. I., Esch, M., Keenlyside, N., Kornblueh, L., Luo, J.-J., and Yamagata, T.: How May Tropical Cyclones Change in a Warmer Climate?, Tellus A: Dynamic Meteorology and Oceanography, 59, 2007.

Benjamini, Y. and Hochberg, Y.: Controlling the False Discovery Rate: A Practical and Powerful Approach to Multiple Testing, Journal of the Royal Statistical Society: Series B (Methodological), 57, 289–300, https://doi.org/10.1111/j.2517-6161.1995.tb02031.x, 1995.

Brönnimann, S., Franke, J., Valler, V., Hand, R., Samakinwa, E., Lundstad, E., Burgdorf, A.-M., Lipfert, L., Pfister, L., Imfeld, N., and Rohrer, M.: Past Hydroclimate Extremes in Europe Driven by Atlantic Jet Stream and Recurrent Weather Patterns, Nature Geoscience, 18, 246–253, https://doi.org/10.1038/s41561-025-01654-y, 2025.

https://doi.org/10.5194/egusphere-2026-1045
Preprint. Discussion started: 10 March 2026

Buehler, T., Raible, C. C., and Stocker, T. F.: The Relationship of Winter Season North Atlantic Blocking Frequencies to Extreme Cold or Dry Spells in the ERA-40, Tellus A, 63, 212–222, https://doi.org/10.1111/j.1600-0870.2010.00492.x, 2011.

Bukenberger, M., Rüdisühli, S., and Schemm, S.: Jet Stream Dynamics from a Potential Vorticity Gradient Perspective: The Method and Its Application to a Kilometre-Scale Simulation, Quarterly Journal of the Royal Meteorological Society, 149, 2409–2432, https://doi.org/10.1002/qj.4513, 2023.

Cassou, C., Terray, L., and Phillips, A. S.: Tropical Atlantic Influence on European Heat Waves, Journal of Climate, 18, 2805–2811, https://doi.org/10.1175/JCLI3506.1, 2005.

Coumou, D., Lehmann, J., and Beckmann, J.: The Weakening Summer Circulation in the Northern Hemisphere Mid-Latitudes, Science, 348, 324–327, https://doi.org/10.1126/science.1261768, 2015.

Dacre, H. F. and Pinto, J. G.: Serial Clustering of Extratropical Cyclones: A Review of Where, When and Why It Occurs, npj Climate and Atmospheric Science, 3, 48, https://doi.org/10.1038/s41612-020-00152-9, 2020.

Davies, H. C.: An Interpretation of Sudden Warmings In Terms of Potential Vorticity, Journal of the Atmospheric Sciences, 38, 427–445, https://doi.org/10.1175/1520-0469(1981)038<0427:AIOSWI>2.0.CO;2, 1981.

Dima, I. M. and Wallace, J. M.: On the Seasonality of the Hadley Cell, 2003.

Drouard, M. and Woollings, T.: Contrasting Mechanisms of Summer Blocking Over Western Eurasia, Geophysical Research Letters, 45, 12,040–12,048, https://doi.org/10.1029/2018GL079894, 2018.

Drouard, M., Kornhuber, K., and Woollings, T.: Disentangling Dynamic Contributions to Summer 2018 Anomalous Weather Over Europe, Geophysical Research Letters, 46, 12 537–12 546, https://doi.org/10.1029/2019GL084601, 2019.

Faranda, D., Messori, G., and Yiou, P.: Dynamical Proxies of North Atlantic Predictability and Extremes, Scientific Reports, 7, 41 278, https://doi.org/10.1038/srep41278, 2017.

Frank, W. M.: The Structure and Energetics of the Tropical Cyclone I. Storm Structure, Monthly Weather Review, 105, 1119–1135, https://doi.org/10.1175/1520-0493(1977)105<1119:TSAEOT>2.0.CO;2, 1977.

Franzke, C., Lee, S., and Feldstein, S. B.: Is the North Atlantic Oscillation a Breaking Wave?, Journal of the Atmospheric Sciences, 61, 145–160, https://doi.org/10.1175/1520-0469(2004)061<0145:ITNAOA>2.0.CO;2, 2004.

Franzke, C., Woollings, T., and Martius, O.: Persistent Circulation Regimes and Preferred Regime Transitions in the North Atlantic, Journal of the Atmospheric Sciences, 68, 2809–2825, https://doi.org/10.1175/JAS-D-11-046.1, 2011.

Galfi, V. M. and Messori, G.: Persistent Anomalies of the North Atlantic Jet Stream and Associated Surface Extremes over Europe, Environmental Research Letters, 18, 024 017, https://doi.org/10.1088/1748-9326/acaedf, 2023.

García-Burgos, M., Ayarzagüena, B., Barriopedro, D., and García-Herrera, R.: Jet Configurations Leading to Extreme Winter Temperatures Over Europe, Journal of Geophysical Research: Atmospheres, 128, e2023JD039 304, https://doi.org/10.1029/2023JD039304, 2023.

García-Herrera, R., Díaz, J., Trigo, R. M., Luterbacher, J., and Fischer, E. M.: A Review of the European Summer Heat Wave of 2003, Critical Reviews in Environmental Science and Technology, 40, 267–306, https://doi.org/10.1080/10643380802238137, 2010.

Gerber and Vallis: Eddy–Zonal Flow Interactions and the Persistence of the Zonal Index, 2007.

Grams, C. M., Beerli, R., Pfenninger, S., Staffell, I., and Wernli, H.: Balancing Europe's Wind-Power Output through Spatial Deployment Informed by Weather Regimes, Nature Climate Change, 7, 557–562, https://doi.org/10.1038/nclimate3338, 2017.

Harnik, N., Garfinkel, C. I., and Lachmy, O.: The Influence of Jet Stream Regime on Extreme Weather Events, in: Dynamics and Predictability of Large-Scale, High-Impact Weather and Climate Events, edited by Li, J., Swinbank, R., Grotjahn, R., and

https://doi.org/10.5194/egusphere-2026-1045
Preprint. Discussion started: 10 March 2026

Volkert, H., pp. 79–94, Cambridge University Press, 1 edn., ISBN 978-1-107-77554-1 978-1-107-07142-1 978-1-107-41680-2, https://doi.org/10.1017/CBO9781107775541.007, 2016.

Hartmann, D. L.: The Atmospheric General Circulation and Its Variability, Journal of the Meteorological Society of Japan. Ser. II, 85B, 123–143, https://doi.org/10.2151/jmsj.85B.123, 2007.

Hersbach, H., Bell, B., Berrisford, P., Hirahara, S., Horányi, A., Muñoz-Sabater, J., Nicolas, J., Peubey, C., Radu, R., Schepers, D., Simmons, A., Soci, C., Abdalla, S., Abellan, X., Balsamo, G., Bechtold, P., Biavati, G., Bidlot, J., Bonavita, M., De Chiara, G., Dahlgren, P., Dee, D., Diamantakis, M., Dragani, R., Flemming, J., Forbes, R., Fuentes, M., Geer, A., Haimberger, L., Healy, S., Hogan, R. J., Hólm, E., Janisková, M., Keeley, S., Laloyaux, P., Lopez, P., Lupu, C., Radnoti, G., de Rosnay, P., Rozum, I., Vamborg, F., Villaume, S., and Thépaut, J.-N.: The ERA5 Global Reanalysis, Quarterly Journal of the Royal Meteorological Society, 146, 1999–2049, https://doi.org/10.1002/qj.3803, 2020.

Hoskins, B. J.: Fluid Dynamics of the Mid-Latitude Atmosphere, 2014.

Hoskins, B. J. and Valdes, P. J.: On the Existence of Storm-Tracks, Journal of the Atmospheric Sciences, 47, 1854–1864, https://doi.org/10.1175/1520-0469(1990)047<1854:OTEOST>2.0.CO;2, 1990.

Jekel, C. F., Venter, G., Venter, M. P., Stander, N., and Haftka, R. T.: Similarity Measures for Identifying Material Parameters from Hysteresis Loops Using Inverse Analysis, International Journal of Material Forming, 12, 355–378, https://doi.org/10.1007/s12289-018-1421-8, 2019.

Kaderli, S.: Skaderli/WaveBreaking: WaveBreaking v0.3.8, Zenodo, https://doi.org/10.5281/zenodo.14214463, 2024.

Kopp, J., Rivoire, P., Ali, S. M., Barton, Y., and Martius, O.: A Novel Method to Identify Sub-Seasonal Clustering Episodes of Extreme Precipitation Events and Their Contributions to Large Accumulation Periods, Hydrology and Earth System Sciences, 25, 5153–5174, https://doi.org/10.5194/hess-25-5153-2021, 2021.

Limbach, S., Schömer, E., and Wernli, H.: Detection, Tracking and Event Localization of Jet Stream Features in 4-D Atmospheric Data, Geoscientific Model Development, 5, 457–470, https://doi.org/10.5194/gmd-5-457-2012, 2012.

Madden, R. A. and Julian, P. R.: Description of Global-Scale Circulation Cells in the Tropics with a 40–50 Day Period, Journal of the Atmospheric Sciences, 29, 1109–1123, https://doi.org/10.1175/1520-0469(1972)029<1109:DOGSCC>2.0.CO;2, 1972.

Maddison, J. W., Ayarzagüena, B., Barriopedro, D., and García-Herrera, R.: Added Value of a Multiparametric Eddy-Driven Jet Diagnostic for Understanding European Air Stagnation, Environmental Research Letters, 18, 084 022, https://doi.org/10.1088/1748-9326/ace72e, 2023.

Martius, O.: A Lagrangian Analysis of the Northern Hemisphere Subtropical Jet, https://doi.org/10.1175/JAS-D-13-0329.1, 2014.

Martius, O. and Wernli, H.: A Trajectory-Based Investigation of Physical and Dynamical Processes That Govern the Temporal Evolution of the Subtropical Jet Streams over Africa, Journal of the Atmospheric Sciences, 69, 1602–1616, https://doi.org/10.1175/JAS-D-11-0190.1, 2012.

Martius, O., Schwierz, C., and Davies, H. C.: Breaking Waves at the Tropopause in the Wintertime Northern Hemisphere: Climatological Analyses of the Orientation and the Theoretical LC1/2 Classification, Journal of the Atmospheric Sciences, 64, 2576–2592, https://doi.org/10.1175/JAS3977.1, 2007.

Martius, O., Schwierz, C., and Davies, H. C.: Tropopause-Level Waveguides, Journal of the Atmospheric Sciences, 67, 866–879, https://doi.org/10.1175/2009JAS2995.1, 2010.

McIntyre, M. E. and Palmer, T. N.: Breaking Planetary Waves in the Stratosphere, Nature, 305, 593–600, https://doi.org/10.1038/305593a0, 1983.

https://doi.org/10.5194/egusphere-2026-1045
Preprint. Discussion started: 10 March 2026

Menzel, M. E., Waugh, D., and Grise, K.: Disconnect Between Hadley Cell and Subtropical Jet Variability and Response to Increased CO2, Geophysical Research Letters, 46, 7045–7053, https://doi.org/10.1029/2019GL083345, 2019.

Messori, G. and Caballero, R.: On Double Rossby Wave Breaking in the North Atlantic, Journal of Geophysical Research: Atmospheres, 120, 11,129–11,150, https://doi.org/10.1002/2015JD023854, 2015.

Messori, G., Caballero, R., and Faranda, D.: A Dynamical Systems Approach to Studying Midlatitude Weather Extremes: Dynamical Systems for Weather Extremes, Geophysical Research Letters, 44, 3346–3354, https://doi.org/10.1002/2017GL072879, 2017.

Nakamura, N. and Huang, C. S. Y.: Atmospheric Blocking as a Traffic Jam in the Jet Stream, Science, 361, 42–47, https://doi.org/10.1126/science.aat0721, 2018.

Pappert, D., Tuel, A., Coumou, D., Vrac, M., and Martius, O.: Long vs. Short: Understanding the Dynamics of Persistent Summer Hot Spells in Europe, Weather and Climate Dynamics, 6, 769–788, https://doi.org/10.5194/wcd-6-769-2025, 2025.

Peyrillé, P., Lafore, J.-P., and Boone, A.: The Annual Cycle of the West African Monsoon in a Two-Dimensional Model: Mechanisms of the Rain-Band Migration, Quarterly Journal of the Royal Meteorological Society, 142, 1473–1489, https://doi.org/10.1002/qj.2750, 2016.

Pinto, J. G., Gómara, I., Masato, G., Dacre, H. F., Woollings, T., and Caballero, R.: Large-Scale Dynamics Associated with Clustering of Extratropical Cyclones Affecting Western Europe, Journal of Geophysical Research: Atmospheres, 119, 13,704–13,719, https://doi.org/10.1002/2014JD022305, 2014.

Priestley, M. D. K., Pinto, J. G., Dacre, H. F., and Shaffrey, L. C.: Rossby Wave Breaking, the Upper Level Jet, and Serial Clustering of Extratropical Cyclones in Western Europe: WESTERN EUROPE CLUSTERING DYNAMICS, Geophysical Research Letters, 44, 514–521, https://doi.org/10.1002/2016GL071277, 2017.

Rivière, G.: Effect of Latitudinal Variations in Low-Level Baroclinicity on Eddy Life Cycles and Upper-Tropospheric Wave-Breaking Processes, Journal of the Atmospheric Sciences, 66, 1569–1592, https://doi.org/10.1175/2008JAS2919.1, 2009.

Robinson, W. A.: On the Self-Maintenance of Midlatitude Jets, Journal of the Atmospheric Sciences, 63, 2109–2122, https://doi.org/10.1175/JAS3732.1, 2006.

Röthlisberger, M., Pfahl, S., and Martius, O.: Regional-Scale Jet Waviness Modulates the Occurrence of Midlatitude Weather Extremes: JET WAVINESS AND WEATHER EXTREMES, Geophysical Research Letters, 43, 10,989–10,997, https://doi.org/10.1002/2016GL070944, 2016.

Rousi, E., Kornhuber, K., Beobide-Arsuaga, G., Luo, F., and Coumou, D.: Accelerated Western European Heatwave Trends Linked to More-Persistent Double Jets over Eurasia, Nature Communications, 13, 3851, https://doi.org/10.1038/s41467-022-31432-y, 2022.

Rupp, P. and Birner, T.: Tropospheric Eddy Feedback to Different Stratospheric Conditions in Idealised Baroclinic Life Cycles, Weather and Climate Dynamics, 2, 111–128, https://doi.org/10.5194/wcd-2-111-2021, 2021.

Schaller, N., Kay, A. L., Lamb, R., Massey, N. R., van Oldenborgh, G. J., Otto, F. E. L., Sparrow, S. N., Vautard, R., Yiou, P., Ashpole, I., Bowery, A., Crooks, S. M., Haustein, K., Huntingford, C., Ingram, W. J., Jones, R. G., Legg, T., Miller, J., Skeggs, J., Wallom, D., Weisheimer, A., Wilson, S., Stott, P. A., and Allen, M. R.: Human Influence on Climate in the 2014 Southern England Winter Floods and Their Impacts, Nature Climate Change, 6, 627–634, https://doi.org/10.1038/nclimate2927, 2016.

Schubert, S., Wang, H., and Suarez, M.: Warm Season Subseasonal Variability and Climate Extremes in the Northern Hemisphere: The Role of Stationary Rossby Waves, Journal of Climate, 24, 4773–4792, https://doi.org/10.1175/JCLI-D-10-05035.1, 2011.

Shutts, G. J.: The Propagation of Eddies in Diffluent Jetstreams: Eddy Vorticity Forcing of 'Blocking' Flow Fields, Quarterly Journal of the Royal Meteorological Society, 109, 737–761, https://doi.org/10.1002/qj.49710946204, 1983.

https://doi.org/10.5194/egusphere-2026-1045
Preprint. Discussion started: 10 March 2026

Simmons, A. J. and Hoskins, B. J.: The Life Cycles of Some Nonlinear Baroclinic Waves, Journal of the Atmospheric Sciences, 35, 414–432, https://doi.org/10.1175/1520-0469(1978)035<0414:TLCOSN>2.0.CO;2, 1978.

Tamarin-Brodsky, T. and Harnik, N.: The Relation between Rossby Wave-Breaking Events and Low-Level Weather Systems, Weather and Climate Dynamics, 5, 87–108, https://doi.org/10.5194/wcd-5-87-2024, 2024.

Thorncroft, C. D., Hoskins, B. J., and McIntyre, M. E.: Two Paradigms of Baroclinic-Wave Life-Cycle Behaviour, Quarterly Journal of the Royal Meteorological Society, 119, 17–55, https://doi.org/10.1002/qj.49711950903, 1993.

Times, C.: EUROPE Heatwave, Floods Kill, Canberra Times, p. 5, 1982.

Trouet, V., Babst, F., and Meko, M.: Recent Enhanced High-Summer North Atlantic Jet Variability Emerges from Three-Century Context, Nature Communications, 9, 180, https://doi.org/10.1038/s41467-017-02699-3, 2018.

Tuel, A. and Martius, O.: Weather Persistence on Sub-Seasonal to Seasonal Timescales: A Methodological Review, Earth System Dynamics, 14, 955–987, https://doi.org/10.5194/esd-14-955-2023, 2023.

Vautard, R.: Multiple Weather Regimes over the North Atlantic: Analysis of Precursors and Successors, Monthly Weather Review, 118, 2056–2081, https://doi.org/10.1175/1520-0493(1990)118<2056:MWROTN>2.0.CO;2, 1990.

Vishnupriya, S., Sprenger, M., Joos, H., and Wernli, H.: The Interaction of Warm Conveyor Belt Outflows with the Upper-Level Waveguide: A Four-Type Climatological Classification, Weather and Climate Dynamics, 6, 1195–1219, https://doi.org/10.5194/wcd-6-1195-2025, 2025.

Wang, M., Huang, Y., Franzke, C. L. E., Yuan, N., Fu, Z., and Boers, N.: Evidence for Preferred Propagating Terrestrial Heatwave Pathways Due to Rossby Wave Activity, Nature Communications, 16, 4742, https://doi.org/10.1038/s41467-025-60104-w, 2025.

Wernli, H. and Gray, S. L.: The Importance of Diabatic Processes for the Dynamics of Synoptic-Scale Extratropical Weather Systems – a Review, Weather and Climate Dynamics, 5, 1299–1408, https://doi.org/10.5194/wcd-5-1299-2024, 2024.

White, R. H., Kornhuber, K., Martius, O., and Wirth, V.: From Atmospheric Waves to Heatwaves: A Waveguide Perspective for Understanding and Predicting Concurrent, Persistent, and Extreme Extratropical Weather, Bulletin of the American Meteorological Society, 103, E923–E935, https://doi.org/10.1175/BAMS-D-21-0170.1, 2022.

Wilks, D. S.: "The Stippling Shows Statistically Significant Grid Points": How Research Results Are Routinely Overstated and Overinterpreted, and What to Do about It, Bulletin of the American Meteorological Society, 97, 2263–2273, https://doi.org/10.1175/BAMS-D-15-00267.1, 2016.

Winters, A. C. and Martin, J. E.: The Role of a Polar/Subtropical Jet Superposition in the May 2010 Nashville Flood, Weather and Forecasting, 29, 954–974, https://doi.org/10.1175/WAF-D-13-00124.1, 2014.

Wirth, V.: Waveguidability of Idealized Midlatitude Jets and the Limitations of Ray Tracing Theory, Weather and Climate Dynamics, 1, 111–125, https://doi.org/10.5194/wcd-1-111-2020, 2020.

Wirth, V. and Polster, C.: The Problem of Diagnosing Jet Waveguidability in the Presence of Large-Amplitude Eddies, Journal of the Atmospheric Sciences, 78, 3137–3151, https://doi.org/10.1175/JAS-D-20-0292.1, 2021.

Woollings, T., Barnes, E., Hoskins, B., Kwon, Y.-O., Lee, R. W., Li, C., Madonna, E., McGraw, M., Parker, T., Rodrigues, R., Spensberger, C., and Williams, K.: Daily to Decadal Modulation of Jet Variability, Journal of Climate, 31, 1297–1314, https://doi.org/10.1175/JCLI-D-17-0286.1, 2018.

Yamazaki, A. and Itoh, H.: Vortex–Vortex Interactions for the Maintenance of Blocking. Part I: The Selective Absorption Mechanism and a Case Study, Journal of the Atmospheric Sciences, 70, 725–742, https://doi.org/10.1175/JAS-D-11-0295.1, 2013.

Zhang, C.: Madden-Julian Oscillation, Reviews of Geophysics, 43, https://doi.org/10.1029/2004RG000158, 2005.